GENERAL INSTRUCTIONS

- **Authors: Please check ALL author names for correct spelling, abbreviations, and order of first and last name in the byline, affiliation footnote, and bios.**
- **Authors: We cannot accept new source files as corrections for your paper. If possible, please annotate the PDF proof we have sent you with your corrections and upload it via the Author Gateway. Alternatively, you may send us your corrections in list format. You may also upload revised graphics via the Author Gateway.**
- **Authors: Please note that once you click "approve with no changes," the proofing process is now complete and your paper will be sent for final publication and printing. Once your paper is posted on Xplore, it is considered final and the article of record. No further changes will be allowed at this point so please ensure scrutiny of your final proof.**
- **Authors: Unless invited or otherwise informed, a mandatory Excessive Paper Length charges will be incurred if your paper is over the page limit set by the society in the Information for Authors. If you have any questions regarding overlength page charges, need an invoice, or have any other billing questions, please contact reprints@ieee.org as they handle these billing requests.**

QUERIES

Q1. Author: Please confirm or add details for any funding or financial support for the research of this article.
Q2. Author: Please provide the significance of bold entities given in Table I.
Q3. Author: Please check the edits made to the sentence "However, analyzing IC and PA..." for correctness.
Q4. Author: Please provide publisher location for Refs. [16], [49], and [69].
Q5. Author: Please provide page range for Ref. [48].
Q6. Author: Please provide department for Ref. [50].
Q7. Author: Please check whether Ref. [57] is okay as set.
Q8. Author: Please check the edits made to the sentence "He gained international..." for correctness.

Lithium-Ion Battery Degradation Indicators Via Incremental Capacity Analysis

David Anseán, Víctor Manuel García, Manuela González, Cecilio Blanco-Viejo, Juan Carlos Viera, Yoana Fernández Pulido, and Luciano Sánchez

***Abstract*—Lithium-ion battery (LIB) degradation originates from complex mechanisms, usually interacting simultaneously in various degrees of intensity. Due to its complexity, to date, identifying battery aging mechanisms remains challenging. Recent improvements in battery degradation identification have been developed, including validated, *in situ* incremental capacity (IC) and peak area (PA) analysis. Due to their *in situ* and non-destructive nature, IC and PA implementation is feasible in on-board battery management systems (BMSs). Despite their advantages, the understanding and applicability of IC and PA techniques is not straightforward, as it requires both electrochemical and material science backgrounds. However, BMS design teams are mainly integrated by electrical engineers and may not include battery scientists. Aiming to bridge gaps in knowledge between electrical engineering and battery science toward battery degradation identification, here we present a systematic approach consisting in a set of lookup tables generated from IC and PA techniques. The lookup tables provide a simple, yet reliable, tool for the evaluation of LIB degradation modes. Various real-life examples of cell degradation are also presented to illustrate and validate the use of the proposed approach. This study exemplifies the use of lookup tables providing a simple, fast, and accurate automated estimation of LIB degradation modes to be implemented in BMSs.**

***Index Terms*—Battery degradation modes, incremental capacity (IC) analysis, lithium-ion battery (LIB), lookup tables.**

I. Introduction

LITHIUM-ION batteries (LIBs) have become ubiquitous in our society, particularly for its use in consumer electronic devices, such as cell phones, laptops, or tablets [1], [2]. Similarly, in virtue of continuous improvements in battery research, LIBs have also become the power source of choice for sustainable transportation, e.g., electric vehicles (EVs) and hybrid vehicles (HEVs) [3]–[6]. Recently, LIBs are gaining momentum in applications of massive electrical energy storage, i.e., battery energy storage systems (BESS) [7]–[10]. In view of these facts, LIBs are playing a fundamental role globally, both in industrial and commercial applications.

Despite its steady progress, LIB systems still face issues to be addressed, mainly related to degradation and performance [11], and management methods [12], [13]. Indeed, the study of aging and failure mechanisms has developed at a much slower pace than LIB performance [14]. Battery degradation presents a major concern in long-term, reliable applications, including EVs, BESS, and aerospace systems, where long cycle life under demanding duty schemes is required. Similarly, it is equally important to measure and estimate the functional status of the battery and protect it from hazardous conditions. Indeed, different degradation phenomena in LIBs lead to different aging patterns and failure modes [15]. All those critical parameters are to be assessed in the BMS. Therefore, to improve the overall system's capabilities, it becomes essential to both understand and identify the LIB degradation phenomena and integrate these features in BMSs.

To understand and evaluate cell degradation phenomena, numerous techniques—including *in situ* and *postmortem*—have been developed [16]–[18]. Among *in situ* techniques that are feasible in BMS applications, IC and PA are recognized as some of the most advanced, non-invasive techniques to identify LIB degradation modes [19]–[22]. Despite the established advantages of using IC and PA to monitor cell degradation, these analyses usually appear tedious at first, particularly for those unfamiliar with these techniques.

The main disciplines that technically contribute to the assessment of cell degradation (i.e., Material Science–Electrochemistry and Electrical Engineering–Computer Science), do not often interact. An optimal design of LIB systems shall involve both scientists and engineer's collaboration at its core. In addition, a fundamental understanding of each other's background shall be required. The approach behind this concept is shown in Fig. 1, where we aim to illustrate the importance of linking Battery Science and Battery Engineering, to design state-of-the-art, reliable, and efficient battery systems.

Herein, we present a framework to systematically analyze cell degradation via IC and PA via lookup tables. Lookup tables are commonly used in computer science to save processing time,

Manuscript received August 2, 2018; revised October 29, 2018; accepted December 19, 2018. Paper 2018-PEDCC-0553.R1 presented at the 2017 IEEE International Conference on Environment and Electrical Engineering and 2017 IEEE Industrial and Commercial Power Systems Europe, Milan, Italy, Jun. 6–9, and approved for publication in the IEEE Transactions on Industry Applications by the Power Electronic Devices and Components Committee of the IEEE Industry Applications Society. This work was supported in part by the Science and Innovation Ministry and in part by FEDER, under Projects DPI2013-046541-R, TIN2014-56967-R, TEC2016-80700-R (AEI/FEDER, UE), and TIN2017-84804-R. *(Corresponding author: David Anseán.)*

D. Anseán, M. González, C. Blanco-Viejo, J. C. Viera, and Y. F. Pulido are with the Electrical Engineering Department, University of Oviedo, Gijón 33203, Spain (e-mail: anseandavid@uniovi.es; mgonzalez@uniovi.es; cecilio@uniovi.es; viera@uniovi.es; fernandezyoana@uniovi.es).

V. M. García is with the Physical and Analytical Chemistry Department, University of Oviedo, Gijón 33203, Spain (e-mail: victorg@uniovi.es).

L. Sánchez is with the Computer Science Department, University of Oviedo, Gijón 33203, Spain (e-mail: luciano@uniovi.es).

Color versions of one or more of the figures in this paper are available online at http://ieeexplore.ieee.org.

Digital Object Identifier 10.1109/TIA.2019.2891213

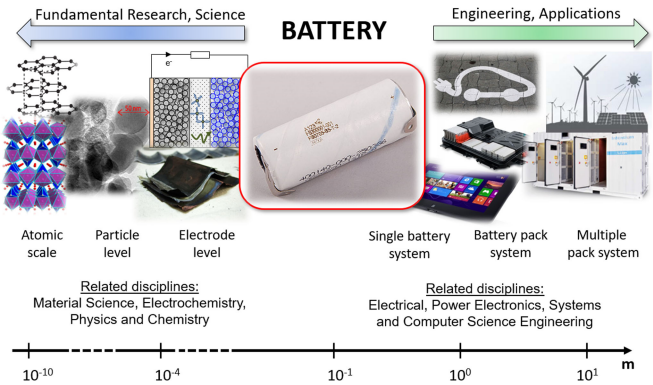

Fig. 1. General perspective of disciplines, background, and system levels that takes place in the design of lithium-ion battery systems.

although the approach is applied in different fields [23]–[25]. In this paper, the lookup tables present the main LIB degradation modes and their relation to IC and PA patterns. The lookup tables avoid extensive and non-straightforward electrochemical analyses, therefore facilitating LIB degradation identification for BMS integration.

We shall begin with a brief background of cell aging mechanisms and IC and PA analysis, then present the lookup tables, and conclude with examples of real LIB experiments, to illustrate the use and applicability of the framework using lookup tables. Due to space constrains, this paper is focused in one LIB cell technology, commonly used graphite‖lithium iron phosphate (GIC‖LFP). However, the high-level methodology presented here is valid for all intercalation LIB materials found in almost every commercial LIB system.

II. Theoretical Background—Cell Aging Mechanisms, Incremental Capacity (IC), and Peak Area (PA) Analysis

A. LIB Aging Mechanisms

Overall, LIBs degrade by capacity and power fade [14]. However, the underpinning phenomenon that originates LIB degradation involves more complex processes. These processes are originated from multiple degradation mechanisms, usually taking place simultaneously [11]. These degradation mechanisms are commonly identified as loss of lithium inventory (LLI), loss of active material (LAM), ohmic resistance increase (ORI), and lithium plating [11], [26], [27].

From the different cell degradation modes, LLI is generally the primary source, leading to direct capacity fade [26], [28]. LLI is a loss of usable Li ions, caused by parasitic reactions that are originated within the cell, and are mainly attributed to the continuous growth of the solid electrolyte interface (SEI) layer [29]. The LAM is related to structural and mechanical degradation of the electrodes [28]. Although LLI can take place alone [30], [31], LAM takes place simultaneously with LLI, as studies indicate [19], [32]–[35]. Recently, LAM has been experimentally demonstrated to have "silent" effects, i.e., degradation that is not exhibited in cell capacity fade [36]. This peculiar "silent" degradation can eventually trigger sudden appearances of rapid capacity loss, known as second degradation stages [26]. Overall, LAM can lead to both capacity and power fade. The ORI causes a shift of the voltage potential of the cell, therefore reducing its energy efficiency. ORI is generally referred as the degradation caused on the electrodes and electrolyte materials that directly result in an increase of the electronic and ionic resistance of a cell. ORI generally results from various sources of cell degradation, including LLI (SEI growth and destabilization [29]) and LAM (e.g., particle isolation, binder decomposition [11]). Lastly, lithium plating is considered as one of the most detrimental degradation modes in LIBs; it increases the rate of cell capacity fade, and may lead to safety issues due to dendrite growth that can internally short circuit the cell [37]. Metallic lithium is highly reactive, thus consuming usable Li ions (i.e., LLI) [34], and further increasing the rate of LLI [11], [36]. Similarly, lithium plating may block pores, isolate active particles and/or delaminate collector, leading to LAM [11], [38], [39]. In-depth analyses on LIB aging mechanisms can be found in reviews [11], [15], [37], [39]–[42], showing the relevance of these phenomena.

B. IC Analysis

The IC analysis identifies cell degradation mechanisms at electrode level. This information, contrary to less advanced, standard battery aging measurements (e.g., internal resistance and capacity fade evaluation), allows accurate battery diagnosis in a time-resolved manner. Another key advantage of IC is the ability to enable battery prognosis, thanks to the identification of the cell aging modes. Finally, a decisive BMS design condition is also accomplished, since the IC is implemented *in situ*. In all, due to these advantages, IC is recognized as a key technique to infer cell degradation, feasible in BMS applications.

Technically, the IC is an *in situ* electrochemical technique that detects the gradual changes in cell behavior, with great sensitivity, by studying the evolution with cycling of the resulting IC curves. The IC analyses are based on the original work by Thompson in 1979 [43], applied to material science research. It was later used in the 1990s by Dahn, to characterize carbon materials for LIB applications [44], and more recently by Dubarry and other groups [20], [21], [26], [45]–[48], to monitor cell degradation avoiding complex *postmortem* analyses.

Mathematically, the IC results from the ratio between an increment of capacity and a fixed voltage increment ($\mathrm{IC} = \Delta Q/\Delta V$). By tracking the increments of capacity associated with the voltage steps, the IC curve is generated. To illustrate the procedure, Fig. 2. is presented; the curve shows the evolution of cell voltage versus the state of charge. A fixed-voltage step (ΔV) yields different capacities (ΔQ_n), as cell voltage evolves. Applying $\mathrm{IC}_n = \Delta Q_n/\Delta V$ yields for this example $\mathrm{IC}_2 > \mathrm{IC}_1 > \mathrm{IC}_3 > \mathrm{IC}_4$. Hence, depending on the cell voltage profile, IC peaks with different intensities are formed. As expected from the mathematical expression, cell voltage plateaus result in large capacity increments (ΔQ_2), which yields large IC peaks. Conversely, abrupt cell voltage changes result in small capacity increments (ΔQ_4).

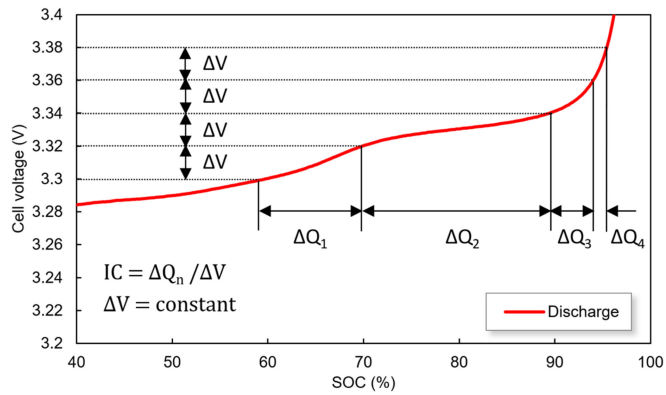

Fig. 2. Graphical representation of the IC values for a given SOC interval in a lithium-ion battery.

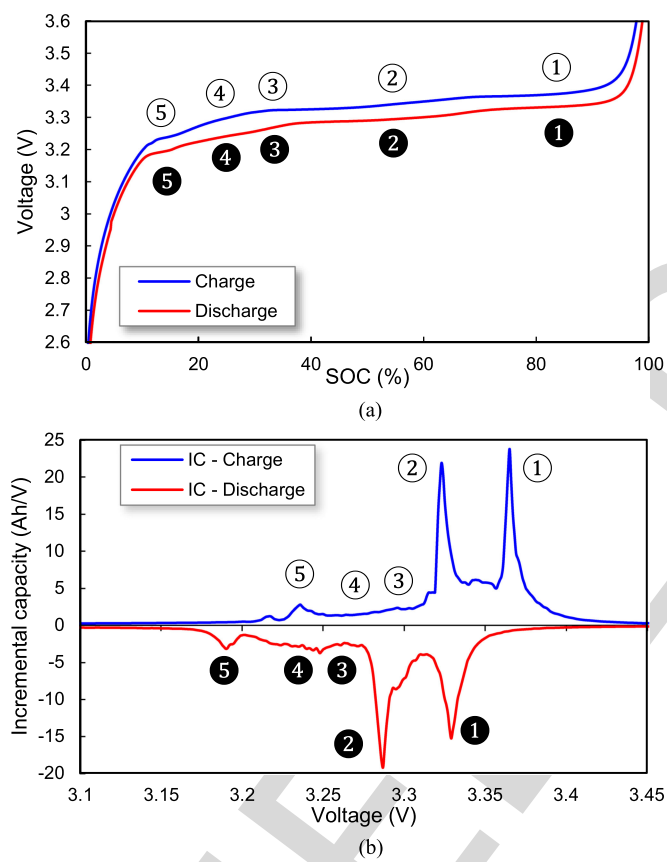

Fig. 3. (a) Charge (blue) and discharge (red) curves of a GIC||LFP cell at C/25. (b) Shows the resulting IC curves.

To better illustrate IC, Fig. 3 is presented: Fig. 3(a) shows the charge/discharge curves of a commercial GIC||LFP cell and Fig. 3(b) shows the resulting IC curves cycled at C/25.

The IC peaks are labeled as (①, ②, ③, ④, and ⑤) for charge, and (❶, ❷, ❸, ❹, and ❺) for discharge. Each IC peak is labeled according to the different electrochemical staging phenomena that take place in the cell [26]. Each IC peak is the result of the convolution of the electrochemical reactions in the active positive and negative electrode materials [49]. That is, the resulting IC peaks contain electrochemical signatures of both electrodes and exhibit a unique shape and intensity. Therefore,

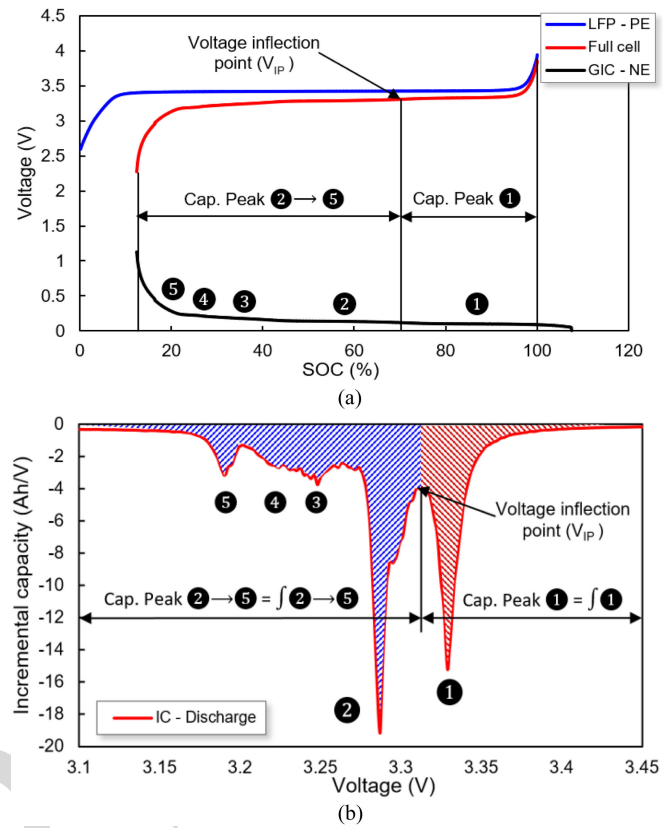

Fig. 4. (a) Discharge curve of a GIC||LFP cell at C/25, showing the individual electrodes (positive, blue, negative, black) and the resulting full cell curve (red). In (b), the schematic representation to obtain the PA is presented.

tracking the evolution of IC peak's shape and position as the cell ages reveals key information on the cell electrochemical phenomena and electrode degradation mechanisms.

C. PA Analysis

PA is a technique derived from the IC, and quantifies the area associated with the phase transformations of a cell. These phase transformations correspond to the formation of solid solutions, and are detected from the IC inflection points [19], [45]. Hence, the PA yields the capacity underneath the IC peaks. This information is used to quantify the degree of degradation within a phase transformation of a LIB.

Fig. 4 presents the PA technique: Fig. 4(a) shows the voltage profile of a commercial GIC||LFP cell (red curve). This voltage is obtained from the subtraction of the positive electrode (blue, LFP) minus the negative electrode (black, graphite). The PA is calculated from the capacity associated underneath the IC peaks [dashed area, see Fig. 4(b)], which correspond to various phase transformations.

For a better detection and quantification of the aging modes in this cell technology, it is recommended to separate the area underneath peak ❶ and the area associated to peaks ❷–❺. This is because the predominant aging mode (i.e., LLI) primarily affects peak ❶ [26], whereas another common degradation mode (i.e., LAM on the NE) affects peaks ❷–❺.

To calculate the area of a peak, i.e., ∫❶, the IC curve [see Fig. 4(b)] is generated. Then, the cell voltage inflection point (V_{IP}) between peak ❶ and ❷ is detected. The inflection point is evaluated versus the cell state of charge [see Fig. 4(a)], yielding ∫❶. Subtracting the full cell capacity minus ∫❶ yields the PA of ❷–❺, i.e., ∫❷–❺. The PA distribution can be directly given in Ah, or in terms of percentage of the total cell capacity (i.e., relative to the SOC).

The evolution of the PA distribution changes as the cell ages according to IC. Hence, tracking the evolution of the PA allows for an *in situ* evaluation of degradation modes from a quantitative perspective (i.e., in Ah), complementing advanced IC diagnosis.

D. Identification of Cell Degradation Via IC and PA Analyses

Degradation mechanisms in LIBs result from various aging modes: LLI, LAM, ORI, and lithium plating. Furthermore, LAM is divided into four degradation modes on the negative electrode (i.e., $\mathrm{LAM_{NE}}$) and/or in the positive electrode (i.e., $\mathrm{LAM_{PE}}$), either on delithiated (de) or lithiated (li) state, giving a total of four aging modes (i.e., $\mathrm{LAM_{deNE}}$, $\mathrm{LAM_{dePE}}$, $\mathrm{LAM_{liNE}}$, and $\mathrm{LAM_{liPE}}$) [26]. Each aging mode affects both the IC and PA curves in a unique manner. Hence, the analysis of each aging mode is required to construct the lookup tables.

As an example to show lookup table construction from IC and PA curves, this subsection presents the most common aging mode (i.e., LLI). The approach presented here is applied to all degradation mechanisms. A comprehensive analysis of each of the aging modes is out of the scope of this paper, and can be found elsewhere [26], [50]. In particular, Birkl *et al.* [28] have made significant progress in this area, providing an experimental proof of degradation modes.

LLI: In LIBs, LLI is described from an electrode perspective as a "slippage," as defined in [26], [51], and [52]. This slippage is described as the mechanisms of which the NE continues to move or shifts toward higher SOCs, while the capacity decreases gradually [53]. The slippage has been experimentally observed and measured in previous works [28], [31], [54], [55], and has also been incorporated in simulation for LIB diagnosis and prognosis analyses [22], [26], [56]. The slippage causes a reduction of IC peak ❶, and its area underneath (i.e., ∫❶), as indicated by arrow ❶ (see Fig. 5). This is because the graphite stage ❶ has been shifted outside the voltage window of the full cell (see Fig. 5, inset figure). Only upon large peak ❶ reduction (i.e., when peak ❶ is extinct), peak ❷ begins to reduce. LLI also causes a slight shift of peak ❺ upon cycling toward high cell potentials. However, its intensity (i.e., ∫❺) is not reduced. Peaks ❸ and ❹ are barely altered by the effect of LLI. Finally, peak ❶ and ❷ voltage inflection point remains constant, although its height is reduced.

The effects of LLI on the PA are shown in Fig. 6(a). As observed, constant rate LLI induces a linear capacity fade of ∫❶, reaching a point where all its capacity is lost (for this example, at cycle 1250). In contrast, ∫❷–❺ evolution remains unaffected, until ∫❶ is extinct. From that point (i.e., cycle 1250), ∫❷–❺ begins to lose capacity linearly. The normalized capacity

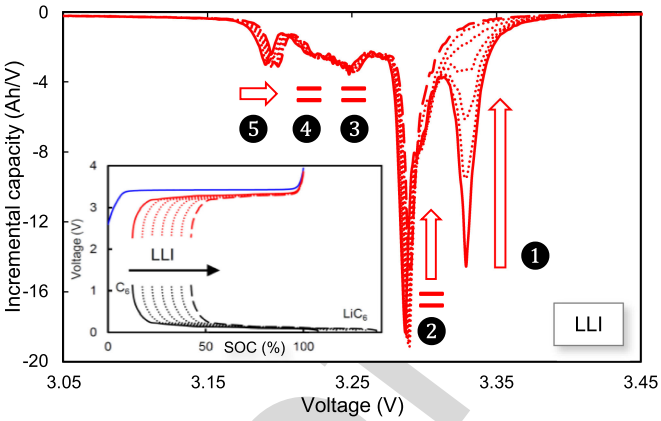

Fig. 5. IC signatures of LLI evolution from beginning (solid line) to end of cycling (dashed). Inset figure shows the NE slippage effect.

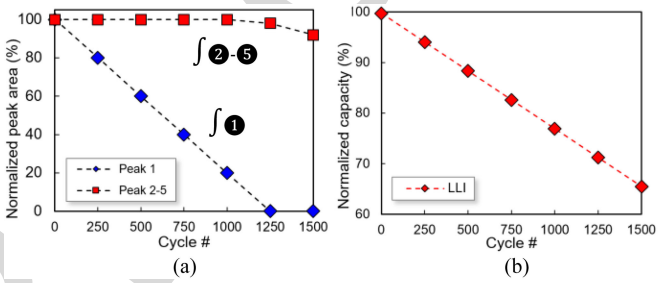

Fig. 6. (a) Normalized PA evolution under LLI for peak 1 (diamond) and peak 2–5 (squared). (b) Capacity fade evolution caused by the effect of LLI alone.

evolution under constant rate LLI induces a linear capacity loss throughout cycling [see Fig. 6(b)].

In brief, LLI mainly affects IC peak ❶ and PA ∫❶. Only under massive cell degradation, ∫❷–❺ is reduced. Peak ❺ can be used as a succinct indicator, tracking its slippage to higher cell voltages. In total, to identify LLI in a GIC‖LFP cell, one should verify peak ❶ and ∫❶ reduction, peak ❺ slippage, while peaks ∫❷–❺ remain unaffected.

III. Experimental

In this paper, we carry out both computer simulations and experimental cell cycle testing. Computer simulations were carried out using the '*alawa* toolbox, developed at the University of Hawaii [26], [57]. Simulations were used to obtain the IC and PA patterns of cell degradation mechanisms (LLI, LAM, ORI, and lithium plating). The model for the computer simulations was constructed using harvested real cell data, as described in [45]. This allows higher accuracy to generate the degradation patterns that are used to construct the lookup tables. Computer simulations were also used to create specific cell evolution patterns.

The experimental procedures were carried out on commercial GIC‖LFP batteries (2.3 Ah), using an Arbint BT-2000 battery tester. For the experiments, a Memmert environmental chamber was used to maintain the cells at 23 °C throughout testing.

To illustrate the usage of the lookup tables, three representative examples of real-life cell capacity evolution patterns are analyzed in this paper. This shall exemplify deciphering cell ag-

TABLE I
LOOKUP TABLE OF MAIN AGING MODES PARTICULARIZED FOR GIC‖LFP CELL DURING DISCHARGE. NOTICE THAT ARROW (↑) INDICATES IC PEAK REDUCTION MAIN FEATURES OF CELL DEGRADATION Q2

Aging modes	Incremental Capacity (peak number)						Peak Area		Cell external and internal constructive parameters				
	❶	❷	❸	❹	❺	⓪	∫❶	∫❷-❺	Capacity fade	Loading ratio	Offset	"Silent"	Risk of plating
LLI	↑	=/↑	=	=	→	=	Decreases/ Depleted	Unchanged/ Decreases	Increases	Unchanged	Increases	No	No
LAM_{deNE}	↓↑	↑	↑	↑	↖	=/=,↓	Increases/ Decreases	Decreases	Unchanged / NL increase or unchanged	Decreases	Unchanged	Yes	Yes
LAM_{liNE}	↑	↑	↑	↑	↗	=	Decreases	Decreases	Increases	Decreases	Increases	No	No
LAM_{dePE}	=/↙	=/↑	=/↑	=/↑	↑	=	Not affected	Unchanged/ NL decreases	Unchanged/ NL increase	Increases	Decreases	Yes	No
LAM_{liPE}	↑	=/↑	=	=	=	=	Decreases/ Depleted	Unchanged/ Decreases	Increases	Increases	Not affected	No	No
ORI	←	←	←	←	←	=	Decreases	Not affected	Increases	Unchanged	Unchanged	No	Yes

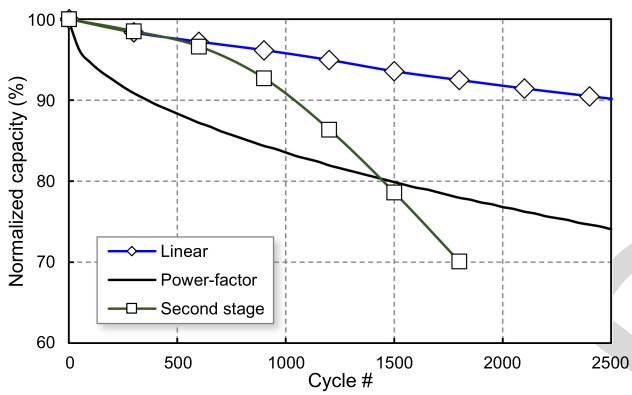

Fig. 7. Normalized capacity versus cycle number for the three most representative cell capacity evolution patterns.

ing modes under realistic scenarios. According to the literature, the most common capacity fade patterns are linear degradation [58]–[60], power-factor degradation [7], [27], [61], and non-linear, second-stage degradation [36], [62], [63].

Fig. 7 shows the three capacity evolution patterns used in this paper. Linear degradation pattern was obtained by continuous constant current cycling, as described in [45]. Power-factor degradation pattern was obtained via '*alawa* toolbox computer simulations, whereas the non-linear, second-stage degradation pattern was obtained by applying dynamic stress cycling, as described in [36]. We shall remark that capacity evolution patterns can give insights on the underlying aging mechanisms, but are not conclusive, since factors, such as temperature, cycling rate, cycling scheme, and/or cell cutoff voltage, modify the rate and shape of the capacity loss trend [36], [38], [41], [55], [63], [64]. Therefore, detailed analyses are to be carried out to decipher the aging modes, regardless of how those trends could be formed.

IV. RESULTS AND DISCUSSION

This section presents the lookup tables and discusses its usage for the three realistic capacity evolution patterns. In brief, each aging mode produces a specific IC and PA signature evolution as the cell ages. However, some aging modes may generate similar IC signatures, complicating its identification. Therefore, it is important to summarize and facilitate the IC and PA evolution for every aging mode, acting individually. These tendencies and features are summarized in the lookup table. As the lookup table is presented, the approach to analyze cell degradation gets simplified: One shall compare the experimental IC and PA results with those generated in the lookup tables, and proceed to evaluate these similarities. The identified change(s) shall correspond to the acting aging mode(s).

A. Lookup Table: IC, PA, and Cell Parameters

Table I presents the lookup table for GIC‖LFP cell technology. The table presents the aging modes (left column), and their effect on IC, PA, and cell external and internal constructive parameters (upper rows) during discharge.

The description of the symbols in the lookup table is as follows: (↑) indicates IC peak reduction and (↓) indicates IC peak increase. The horizontal arrows indicate a voltage shift of the peaks; (→) indicates higher cell voltages, whereas (←) indicates the opposite.

The equal symbol (=) indicates no change in IC patterns. The slash symbol (/) indicates a second degradation stage, i.e., an abrupt change in the capacity evolution pattern [26], [36]. During second degradation stages, the font type is set to red color. The rest of the table is self-described, except "NL" which stands for "non-linear."

Cell external and internal constructive parameter patterns are also described to gain in-depth analysis of the outcomes of the aging modes. External parameters are referred to those that can be directly measured (e.g., capacity fade), whereas internal parameters cannot be directly measured by standard procedures (e.g., cell architecture parameters) [26], [65].

Capacity fade describes the effects that a particular aging mode induces on capacity evolution. The loading ratio (LR) and offset (OFS) describe the stoichiometric cell construction. The LR is the ratio between the capacity contained in the negative and positive electrode (Q_{NE} and Q_{PE}), i.e., LR $= Q_{\mathrm{NE}}/_{\mathrm{PE}}$, as described in [26]. The OFS corresponds to the slippage of the NE over the PE, as previously commented. The table also presents whether the aging mode effect remains "silent" dur-

ing its first degradation stage, therefore indicating why there is no discernible loss of capacity [45]. Finally, the table also includes whether the aging modes can lead to direct lithium plating appearance: Peak ⓪ appearance and growth indicates thermodynamic lithium plating occurrence [36], [66].

In total, the use of the cell constructive parameters is critical for advanced diagnosis and prognosis analyses. In addition, since internal patterns cannot be directly measured, the use of the provided lookup table becomes instrumental. Next sections present further discussion and analyses of these parameters.

B. Use of the Lookup Tables in Real-Life Experiments

Here we illustrate the use of lookup tables to decipher cell aging modes, from real-life experiments. One of the implicit advantages of using lookup tables is their systematic nature; hence, an approach based on various steps can be generated. This approach is based on comparing experimental IC and PA curves versus the lookup tables.

We derive this analysis following the step-by-step process derived from experimental results demonstrated in previous works [19], [28], [36], [45].

1) Generate experimental IC and PA figures.
2) Number all IC peaks (i.e., ❶ to ❺) in the figures.
3) Indicate each IC peak with arrows: Direction, length, and intensity.
4) Analyze peak ❶: Reduction most likely indicates LLI, and to a much lesser degree $\mathrm{LAM_{PE}}$. Initial peak ❶ increase, or initial steady evolution indicates adding effect of $\mathrm{LAM_{deNE}}$.
5) Analyze peaks ❷–❺: Reduction indicates $\mathrm{LAM_{NE}}$, a highly likely scenario. No changes indicate LLI (highly likely) and/or $\mathrm{LAM_{PE}}$ (highly unlikely).
6) Analyze ∫❶ evolution: A reduction equal to the cell capacity fade indicates solely effect of LLI. Initial increase or steady evolution indicates $\mathrm{LAM_{deNE}}$. Reduction indicates $\mathrm{LAM_{liPE}}$ (highly unlikely).
7) Analyze ∫❷–❺ evolution: No changes indicate solely effect of LLI and/or $\mathrm{LAM_{PE}}$ (highly unlikely). Reduction indicates $\mathrm{LAM_{NE}}$.
8) Fine tuning via peak ❺ analysis: Shifting to the right without reduction indicates solely LLI; less intense shifting and reduction, indicates LLI+$\mathrm{LAM_{deNE}}$; intense shifting and reduction, indicates LLI+$\mathrm{LAM_{liNE}}$; $\mathrm{LAM_{PE}}$ affecting peak ❺ is highly unlikely.
9) Other scenarios: ⓪ peak appearance. This peak is associated to $\mathrm{LAM_{deNE}}$ and is related to thermodynamic lithium plating occurrence.

Following the step-by-step process should resolve cell aging modes identification. Further analyses based on literature studies are generally required for improved accuracy for aging mode identification; for example, LAM in the PE for LFP systems is very unlikely, as reported in postmortem analyses [35], [55], [67], [68].

1) Linear Degradation: Fig. 8 shows the IC and PA at C/25 obtained from the cell tested under constant current scheme

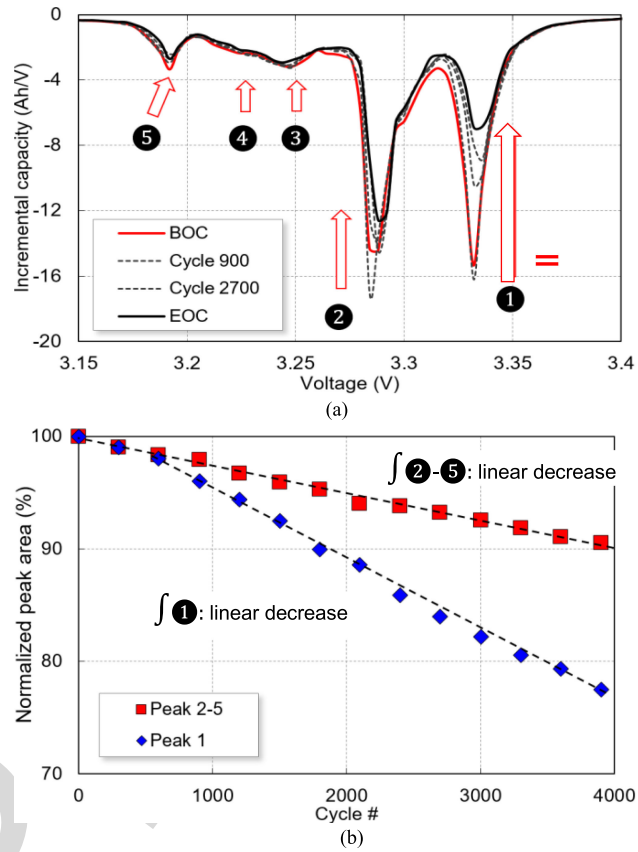

Fig. 8. Linear degradation pattern, and its resulting (a) IC and (b) PA curves.

[45]. The first steps (1–3) are to indicate and label all peaks, as shown in Fig. 8. Then, analyze peak ❶ and ❷–❺, following steps 4 and 5. We deduce that LLI and $\mathrm{LAM_{NE}}$ can be the main aging modes: Peak ❶ reduction accompanied with peak ❷–❺ proportional reduction. From steps 6 and 7, we further corroborate the suggestions: ∫❶ reduction together with ∫❷–❺ linear decrease also indicates LLI+$\mathrm{LAM_{NE}}$.

We now proceed to carry out fine tuning analyses: This shall allow us to separate the aging mode acting on the NE (i.e., $\mathrm{LAM_{deNE}}$ or $\mathrm{LAM_{liNE}}$). The main sensors are peak ❶ and peak ❺. The slight shift of peak ❺ counteracts the shift and reduction that $\mathrm{LAM_{deNE}}$ would produce (see Table I). In addition, peak ❶ reduction does not begin abruptly [see equal symbol in peak ❶ IC curve, see Fig. 8(a)], a fact that also matches with $\mathrm{LAM_{deNE}}$ signature.

The above-mentioned reasoning indicates that aging on the studied cell is caused by LLI (significant reduction of peak ❶), accompanied by the effect of $\mathrm{LAM_{deNE}}$ (reduction of peaks ❷–❺ and slight reduction of peak 1). In addition, due to the larger effects of LLI, we also conclude that aging mode LLI is more prominent than $\mathrm{LAM_{deNE}}$. These results are in agreement with the literature [19], [45].

2) Power Factor Degradation: Fig. 9 shows the IC and PA at C/25, obtained from the cell exhibiting power factor capacity fade, labeling and indicating IC peaks (steps 1–3). According to procedure steps (4–8), this particular example of cell aged under power factor degradation is aged from LLI alone: Only peak ❶

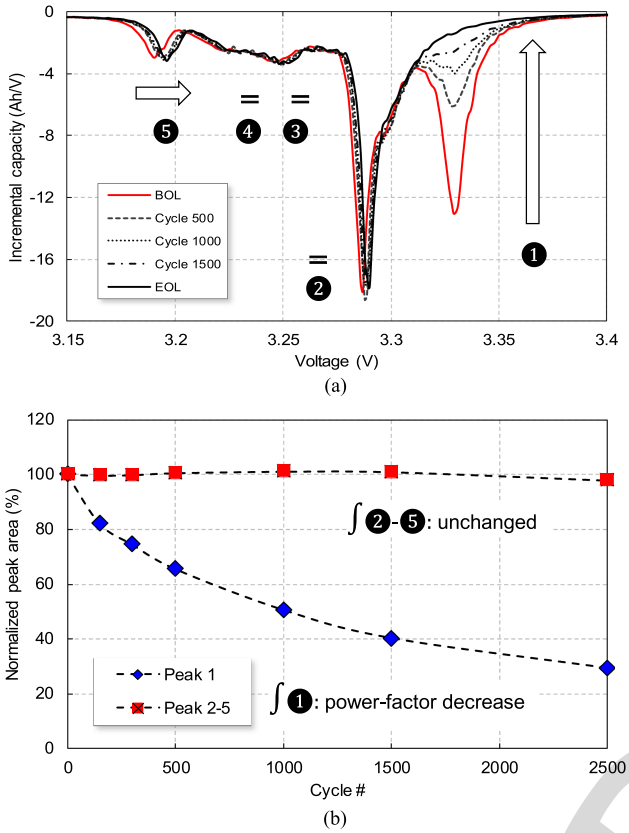

Fig. 9. Power factor degradation pattern, and (a) IC and (b) PA curves.

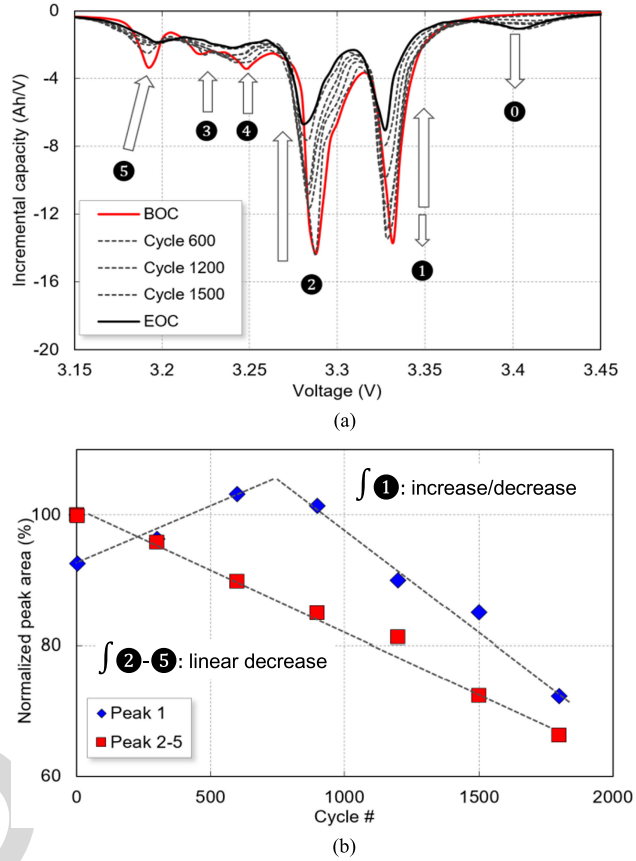

Fig. 10. Dynamic stress cycling, and its resulting (a) IC and (b) PA curves.

is reduced, ❷–❺ peak remains unchanged through cycling, and peak ❺ is shifted significantly toward higher cell voltage, but not reduced (i.e., ∫❺ remains constant).

This type of degradation pattern is generally found (but not exclusive to) in calendar-aged systems [30], [69], systems exposed to high temperatures [70] or systems where the effects of calendar aging are more prominent than those of cycling [61]. Under those conditions, LLI is the major cell aging mode. We shall point out that power factor degradation may not be exclusively caused by LLI, as studies shown [71].

3) Non-linear, Second-Stage Degradation: Fig. 10 shows the IC and PA at C/25 obtained from the cell tested under dynamic stress cycling. In this particular case, degradation seems very complicated at first; IC peaks shifting, reducing, increasing, and even appearing (see peak ⓪). Curiously, these signatures usually facilitate the analysis.

Analyzing steps 4–8 clearly indicates the effect of $\mathrm{LAM_{deNE}}$: Peak ❶ and ∫❶ initial increase, accompanied by peak ∫❷–❺ reduction can only lead to $\mathrm{LAM_{deNE}}$ (see Table I). In addition, LLI is acting to some extent, as peak ❶ and ∫❶ is also reduced, and peak ❺ is shifted to higher cell voltage. However, the most outstanding signature to evaluate cell degradation is the appearance of peak ⓪: This peak can only be derived by the effect of $\mathrm{LAM_{deNE}}$ (see step 9).

From this straightforward analysis, we conclude that the cell is under lithium plating occurrence due to peak ⓪ appearance. In addition, due to the larger effects associated with $\mathrm{LAM_{deNE}}$, we also conclude that aging mode $\mathrm{LAM_{deNE}}$ is more prominent than LLI. These results are in agreement with detailed studies [36], [72], [73].

4) External and Internal Constructive Parameter Analyses: The lookup table can be used to further evaluate cell constructive parameters (see Table I). Deciphering these parameters can lead to improvements in both BMS and cell design processes. Advanced information on lithium plating incubation and/or occurrence can be used in BMSs in various strategies: Modify and reduce the power requirements on the batteries, and/or set a warning state to replace the batteries. These strategies would avoid unnecessary risks of battery degradation or cell failure [36]. This approach also fails in the field of advanced battery prognosis [74], [75]. Tracking the evolution of the OFS and/or the LR can be applied to optimize the mass and area of electrode active materials within the cell for a specific application. The analyses of external and internal parameters illustrate the applicability of the lookup tables in linking both material science and electrical engineering disciplines under common analyses, with mutual objectives in cell and system design improvements.

For the linear degradation pattern, we deciphered LLI and $\mathrm{LAM_{deNE}}$ as the ongoing aging modes. According to Table I, their effects increase the OFS, while reducing LR. In addition, this aging mode combination could lead to lithium plating; however, since the effect of LLI is larger than that of $\mathrm{LAM_{deNE}}$,

this scenario remains unlikely [45]. Interestingly, the effects of $\mathrm{LAM_{deNE}}$ are silent, i.e., cannot be directly estimated from measuring capacity fade. However, analyzing IC and PA allows identifying the silent effect, both from a qualitative (IC), and quantitative (PA) perspective.

The non-linear, second-stage degradation was affected by $\mathrm{LAM_{deNE}}$ and LLI to an extent that induced lithium plating. Verifying the lookup table, the cell reduces its LR (caused by $\mathrm{LAM_{deNE}}$), increases OFS (caused by LLI), shows silent effects (caused by $\mathrm{LAM_{deNE}}$), and is under lithium plating occurrence due to large $\mathrm{LAM_{deNE}}$ effect.

The advantages of using the lookup tables for internal analyses are also exemplified when comparing both linear and non-linear degradation patterns: As observed, during the first 600 cycles (see Fig. 7), both cells show the same capacity fade pattern. Without a proper analysis of the IC and cell constructive parameters, patterns between cells appear identical. However, via IC and lookup table analyses, it is feasible to diagnose and prognose the non-linear, second degradation aging patterns.

5) System-Level Approach: From a system-level perspective, the implementation of the proposed strategy involves various design features to consider. To apply lookup table aging mode identification with highest accuracy, cycling under pseudo-thermodynamic conditions (i.e., C/25) yields optimal results. This slow cycling from reference performance tests (RPTs) can be carried out periodically (i.e., 6–12 mo, depending on the application). We shall point out that EVs or BESS battery packs are designed to last ten years or more of use, specifically BESS with longer life span. Hence, the RPT approach time frame is equivalent to regular maintenance services in other existing energy systems, or internal combustion engine vehicles. Therefore, this strategy shall not present major drawbacks for the overall operation of the system. For consumer electronics, the RPTs could be carried out more often (i.e., 2–4 mo), due to their lower life span. In addition to the high accuracy of C/25 tests, the IC curves obtained under kinetic cycling (i.e., C/2, 1C) can derive useful information to identify polarization resistances and kinetic degradation [20], [45]. These curves can be analyzed regularly, as kinetic cycling is generally found under normal system's usage (i.e., during charges), providing useful ongoing diagnosis information.

Advanced strategies are also being developed to reduce the impact of the maintenance services, aiming to carry out the analyses *in operando*. From a hardware perspective, large systems (i.e., BESS) could disconnect individual power modules to perform dedicated RPTs, without affecting the power capabilities or disconnecting the entire system. From a software perspective, onboard diagnosis using lookup tables with selected features of interest (FOI) of the IC curves can be implemented prior its deployment [66], reducing the need for full charge/discharge cycles. In addition to the above strategies, in future works, we aim to provide advanced approaches to decipher aging *in operando* using transformation models via soft sensors and fuzzy observers [76]. Similarly, future work shall be carried out for algorithm development for the selected BMS platform/architecture.

V. Conclusion

To date, LIB degradation analysis and aging mode identification presents a major concern in long-term, reliable LIB applications. As it becomes essential to integrate these features in state-of-the-art BMSs, this paper presents a systematic approach to identify LIB degradation modes, based on the validated, *in-situ*, IC electrochemical technique. The proposed methodology simplifies the relatively complex and non-straightforward IC analysis procedure, by using a set of inclusive lookup tables and a systematic step-by-step process. This approach is particularly interesting for electrical and system engineers who, despite being the main contributors in BMS design, do not often possess the background to perform this type of electrochemical analyses.

The methodology consists first on individually implementing all LIB degradation modes, analyze their corresponding IC and PA main features, and present them in the form of a lookup table. Then, the lookup table is complemented with a step-by-step procedure to provide a systematic path for LIB degradation identification. The final step consists of obtaining the IC and PA experimental results and following the designed methodology. This shall yield accurate results on LIB aging modes identification. To both validate and exemplify the use of the proposed methodology, we also presented three common, real-life capacity fade scenarios, and deciphered their aging modes.

In a broader perspective, this paper aims to provide a bridge in knowledge between battery science and electrical engineering, with the final objective of using these techniques in novel BMS. The methodology presented here, due to its systematic nature, can be implemented as an algorithm in a microprocessor-based system to be ultimately embedded in the BMS. The prospects of using this set of straightforward tools are attractive to improve BMS designs for battery diagnosis and prognosis.

This approach was applied to GIC‖LFP based batteries. However, the methodology is valid for all intercalation LIBs, which currently represent the vast majority of commercial LIBs. Future work shall focus on specific lookup tables and procedures for various battery chemistries (e.g., nickel manganese oxide, nickel–cobalt–aluminum, etc.). We anticipate that, although the proposed methodology remains unaltered, different IC peaks and FOI will emerge for each particular chemistry. We believe that the availability of the lookup tables in several battery chemistries would create interesting benefits and further discussions in the LIB research community.

References

[1] T. Reddy, *Linden's Handbook of Batteries*, 4th ed. New York, NY, USA: McGraw-Hill, 2011.

[2] G. E. Blomgren, "The development and future of lithium ion batteries," *J. Electrochem. Soc.*, vol. 164, no. 1, pp. A5019–A5025, Dec. 2017.

[3] D. Anseán, V. M. García, M. González, J. C. Viera, J. C. Antón, and C. Blanco, "Evaluation of $LiFePO_4$ batteries for electric vehicle applications," *IEEE Trans. Ind. Appl.*, vol. 51, no. 2, pp. 1855–1863, Mar./Apr. 2015.

[4] X. Gong, R. Xiong, and C. C. Mi, "Study of the characteristics of battery packs in electric vehicles with parallel-connected lithium-ion battery cells," *IEEE Trans. Ind. Appl.*, vol. 51, no. 2, pp. 1872–1879, Mar. 2015.

[5] M. Farhadi and O. Mohammed, "Energy storage technologies for high-power applications," *IEEE Trans. Ind. Appl.*, vol. 52, no. 3, pp. 1953–1961, May 2016.

[6] S. S. Williamson, A. K. Rathore, and F. Musavi, "Industrial electronics for electric transportation: Current state-of-the-art and future challenges," *IEEE Trans. Ind. Electron.*, vol. 62, no. 5, pp. 3021–3032, May 2015.

[7] D. I. Stroe, M. Swierczynski, A. I. Stan, R. Teodorescu, and S. J. Andreasen, "Accelerated lifetime testing methodology for lifetime estimation of lithium-ion batteries used in augmented wind power plants," *IEEE Trans. Ind. Appl.*, vol. 50, no. 6, pp. 4006–4017, Nov./Dec. 2014.

[8] D. I. Stroe, V. Knap, M. Swierczynski, A. I. Stroe, and R. Teodorescu, "Operation of a grid-connected lithium-ion battery energy storage system for primary frequency regulation: A battery lifetime perspective," *IEEE Trans. Ind. Appl.*, vol. 53, no. 1, pp. 430–438, Jan./Feb. 2017.

[9] B. Z. Ma, A. Pesaran, and V. Gevorgian, "Energy storage, renewable power generation, and the grid," *IEEE Electrific. Mag.*, vol. 3, no.3, pp. 30–40, Sep. 2015.

[10] B. Dunn, H. Kamath, and J. M. Tarascon, "Electrical energy storage for the grid: A battery of choices.," *Sci.*, vol. 334, no. 6058, pp. 928–935, Nov. 2011.

[11] J. Vetter *et al.*, "Ageing mechanisms in lithium-ion batteries," *J. Power Sources*, vol. 147, no. 1–2, pp. 269–281, Sep. 2005.

[12] W. Waag, C. Fleischer, and D. U. Sauer, "Critical review of the methods for monitoring of lithium-ion batteries in electric and hybrid vehicles," *J. Power Sources*, vol. 258, pp. 321–339, Jul. 2014.

[13] H. Rahimi-Eichi, U. Ojha, and M.-Y. Chow, "Battery management system—An overview of its application in the smart grid and electric vehicles," *IEEE Ind. Electron. Mag.*, vol. 7, no. 2, pp. 4–16, Jun. 2013.

[14] M. R. Palacín and A. De Guibert, "Batteries: Why do batteries fail?," *Sci.*, vol. 351, no. 6273, p. 1253292, Feb. 2016.

[15] C. Hendricks, N. Williard, S. Mathew, and M. Pecht, "A failure modes, mechanisms, and effects analysis (FMMEA) of lithium-ion batteries," *J. Power Sources*, vol. 297, pp. 113–120, Nov. 2015.

[16] M. Berecibar, I. Gandiaga, I. Villarreal, N. Omar, J. Van Mierlo, and P. Van Den Bossche, "Critical review of state of health estimation methods of Li-ion batteries for real applications," in *Renewable and Sustainable Energy Reviews*, vol. 56. Elsevier, pp. 572–587, 2016.

Q4 [17] P. P. R. M. L. Harks, F. M. Mulder, and P. H. L. Notten, "In situ methods for Li-ion battery research: A review of recent developments," *J. Power Sources*, vol. 288, pp. 92–105, Aug. 2015.

[18] B. Xu, A. Oudalov, A. Ulbig, G. Andersson, and D. S. Kirschen, "Modeling of lithium-ion battery degradation for cell life assessment," *IEEE Trans. Smart Grid*, vol. 9, no. 2, pp. 1131–1140, Mar. 2018.

[19] M. Dubarry, C. Truchot, and B. Y. Liaw, "Cell degradation in commercial $LiFePO_4$ cells with high-power and high-energy designs," *J. Power Sources*, vol. 258, pp. 408–419, Feb. 2014.

[20] M. Dubarry and B. Y. Liaw, "Identify capacity fading mechanism in a commercial $LiFePO_4$ cell," *J. Power Sources*, vol. 194, no. 1, pp. 541–549, Oct. 2009.

[21] M. Berecibar, M. Dubarry, I. Villarreal, N. Omar, and J. Van Mierlo, "Degradation mechanisms detection for HP and HE NMC cells based on incremental capacity curves," in *Proc. IEEE Veh. Power Propulsion Conf.*, pp. 1–5, Oct. 2016.

[22] X. Han, M. Ouyang, L. Lu, J. Li, Y. Zheng, and Z. Li, "A comparative study of commercial lithium ion battery cycle life in electrical vehicle: Aging mechanism identification," *J. Power Sources*, vol. 251, pp. 38–54, Apr. 2014.

[23] R. Xiong, H. He, F. Sun, and K. Zhao, "Evaluation on state of charge estimation of batteries with adaptive extended Kalman filter by experiment approach," *IEEE Trans. Veh. Technol.*, vol. 62, no. 1, pp. 108–117, Jan. 2013.

[24] T. Inoue, S. Miyazaki, and H. Fujiwara, "Universal fault diagnosis for lookup table FPGAs," *IEEE Des. Test Comput.*, vol. 15, no. 1, pp. 39–44, 1998.

[25] A. Heydari, "Revisiting approximate dynamic programming and its convergence," *IEEE Trans. Cybern.*, vol. 44, no. 12, pp. 2733–2743, Dec. 2014.

[26] M. Dubarry, C. Truchot, and B. Y. Liaw, "Synthesize battery degradation modes via a diagnostic and prognostic model," *J. Power Sources*, vol. 219, pp. 204–216, Dec. 2012.

[27] M. Broussely *et al.*, "Main aging mechanisms in Li ion batteries," *J. Power Sources*, vol. 146, no. 1–2, pp. 90–96, Aug. 2005.

[28] C. R. Birkl, M. R. Roberts, E. McTurk, P. G. Bruce, and D. A. Howey, "Degradation diagnostics for lithium ion cells," *J. Power Sources*, vol. 341, pp. 373–386, Feb. 2017.

[29] P. Verma, P. Maire, and P. Novák, "A review of the features and analyses of the solid electrolyte interphase in Li-ion batteries," *Electrochim. Acta*, vol. 55, no. 22, pp. 6332–6341, 2010.

[30] M. Kassem and C. Delacourt, "Postmortem analysis of calendar-aged graphite/$LiFePO_4$ cells," *J. Power Sources*, vol. 235, pp. 159–171, Aug. 2013.

[31] P. Keil and A. Jossen, "Calendar aging of NCA lithium-ion batteries investigated by differential voltage analysis and coulomb tracking," *J. Electrochem. Soc.*, vol. 164, no. 1, pp. A6066–A6074, Oct. 2017.

[32] M. Kerlau, M. Marcinek, V. Srinivasan, and R. M. Kostecki, "Studies of local degradation phenomena in composite cathodes for lithium-ion batteries," *Electrochim. Acta*, vol. 52, no. 17, pp. 5422–5429, May 2007.

[33] D. P. Abraham, J. L. Knuth, D. W. Dees, I. Bloom, and J. P. Christophersen, "Performance degradation of high-power lithium-ion cells—Electrochemistry of harvested electrodes," *J. Power Sources*, vol. 170, no. 2, pp. 465–475, Jul. 2007.

[34] P. Arora, R. White, and M. Doyle, "Capacity fade mechanisms and side reactions in lithium-ion batteries," *J. Electrochem. Soc.*, vol. 145, no. 10, pp. 3647–3667, 1998.

[35] P. Liu *et al.*, "Aging mechanisms of $LiFePO_4$ batteries deduced by electrochemical and structural analyses," *J. Electrochem. Soc.*, vol. 157, no. 4, pp. A499–A507, 2010.

[36] D. Anseán *et al.*, "Operando lithium plating quantification and early detection of a commercial LiFePO4 cell cycled under dynamic driving schedule," *J. Power Sources*, vol. 356, pp. 36–46, 2017.

[37] Q. Liu *et al.*, "Understanding undesirable anode lithium plating issues in lithium-ion batteries," *RSC Adv.*, vol. 6, no. 91, pp. 88683–88700, 2016.

[38] J. C. Burns *et al.*, "Predicting and extending the lifetime of Li-ion batteries," *J. Electrochem. Soc.*, vol. 160, no. 9, pp. A1451–A1456, Jul. 2013.

[39] V. Agubra and J. Fergus, "Lithium Ion battery anode aging mechanisms," *Mater. (Basel).*, vol. 6, no. 4, pp. 1310–1325, Mar. 2013.

[40] A. Barré, B. Deguilhem, S. Grolleau, M. Gérard, F. Suard, and D. Riu, "A review on lithium-ion battery ageing mechanisms and estimations for automotive applications," *J. Power Sources*, vol. 241, pp. 680–689, Nov. 2013.

[41] T. Waldmann, B.-I. Hogg, and M. Wohlfahrt-Mehrens, "Li plating as unwanted side reaction in commercial Li-ion cells—A review," *J. Power Sources*, vol. 384, pp. 107–124, Apr. 2018.

[42] Z. Li, J. Huang, B. Y. Liaw, V. Metzler, and J. Zhang, "A review of lithium deposition in lithium-ion and lithium metal secondary batteries," *J. Power Sources*, vol. 254, pp. 168–182, May 2014.

[43] A. H. Thompson, "Electrochemical potential spectroscopy: A new electrochemical measurement," *J. Electrochem. Soc.*, vol. 126, no. 4, pp. 608–616, Apr. 1979.

[44] Y. Gao and J. R. Dahn, "Synthesis and characterization of LiMnO for Li-ion battery applications," *J. Electrochem. Soc.*, vol. 143, no. 1, pp. 100–114, 1996.

[45] D. Anseán *et al.*, "Fast charging technique for high power LiFePO4 batteries: A mechanistic analysis of aging," *J. Power Sources*, vol. 321, pp. 201–209, Jul. 2016.

[46] M. Safari and C. Delacourt, "Aging of a commercial graphite/LiFePO4 cell," *J. Electrochem. Soc.*, vol. 158, no. 10, pp. A1123–1135, 2011.

[47] M. Dubarry, V. Svoboda, R. Hwu, and B. Y. Liaw, "Incremental capacity analysis and close-to-equilibrium OCV measurements to quantify capacity fade in commercial rechargeable lithium batteries," *Electrochem. Solid-State Lett.*, vol. 9, no. 10, pp. A454–A457, 2006.

[48] D. Anseán, M. González, C. Blanco, J. C. Viera, Y. Fernández, and V. M. García, "Lithium-ion battery degradation indicators via incremental capacity analysis," in *Proc. Conf. Proc.—17th IEEE Int. Conf. Environ. Electr. Eng.1st IEEE Ind. Commercial Power Syst. Europe*, 2017. Q5

[49] B. Y. Liaw and M. Dubarry, *Electric and Hybrid Vehicles, Power Sources, Models, Sustainability, Infrastructure and the Market*. Elsevier, 2010.

[50] D. Anseán, "High power Lithium-ion battery performance: A mechanistic analysis of aging," Ph.D. dissertation, University of Oviedo, Spain, 2015. Q6

[51] J. Christensen and J. Newman, "Cyclable lithium and capacity loss in Li-ion cells," *J. Electrochem. Soc.*, vol. 152, no. 4, pp. A818–A829, 2005.

[52] A. J. Smith, H. M. Dahn, J. C. Burns, and J. R. Dahn, "Long-term low-rate cycling of $LiCoO_2$ /Graphite Li-Ion cells at 55 °C," *J. Electrochem. Soc.*, vol. 159, no. 6, pp. A705–A710, 2012.

[53] M. Dubarry *et al.*, "Evaluation of commercial lithium-ion cells based on composite positive electrode for plug-in hybrid electric vehicle (PHEV) applications: IV. Over-discharge phenomena," *J. Electrochem. Soc.*, vol. 162, no. 9, pp. A1787–A1792, 2015.

[54] A. J. Smith, N. N. Sinha, and J. R. Dahn, "Narrow range cycling and storage of commercial Li Ion cells," *J. Electrochem. Soc.*, vol. 160, no. 2, pp. A235–A242, 2012.

[55] M. Klett *et al.*, "Non-uniform aging of cycled commercial LiFePO4//graphite cylindrical cells revealed by post-mortem analysis," *J. Power Sources*, vol. 257, pp. 126–137, Feb. 2014.

[56] H. M. Dahn, A. J. Smith, J. C. Burns, D. A. Stevens, and J. R. Dahn, "User-friendly differential voltage analysis freeware for the analysis of degradation mechanisms in Li-Ion batteries," *J. Electrochem. Soc.*, vol. 159, no. 9, pp. A1405–A1409, Aug. 2012.

Q7 [57] Alawa Central. (2017). [Online]. Available: https://www.soest.hawaii.edu/HNEI/alawa/

[58] D. Anseán, M. González, J. C. Viera, V. M. García, C. Blanco, and M. Valledor, "Fast charging technique for high power lithium iron phosphate batteries: A cycle life analysis," *J. Power Sources*, vol. 239, pp. 9–15, 2013.

[59] J. Schmalstieg, S. Käbitz, M. Ecker, and D. U. Sauer, "A holistic aging model for Li(NiMnCo)O_2 based 18650 lithium-ion batteries," *J. Power Sources*, vol. 257, pp. 325–334, Jul. 2014.

[60] M. Ecker *et al.*, "Calendar and cycle life study of Li(NiMnCo)O2-based 18650 lithium-ion batteries," *J. Power Sources*, vol. 248, pp. 839–851, Feb. 2014.

[61] J. Wang *et al.*, "Degradation of lithium ion batteries employing graphite negatives and nickel–cobalt–manganese oxide + spinel manganese oxide positives: Part 1, aging mechanisms and life estimation," *J. Power Sources*, vol. 269, pp. 937–948, Dec. 2014.

[62] S. F. Schuster *et al.*, "Nonlinear aging characteristics of lithium-ion cells under different operational conditions," *J. Energy Storage*, vol. 1, pp. 44–53, Jun. 2015.

[63] P. Keil and A. Jossen, "Charging protocols for lithium-ion batteries and their impact on cycle life—An experimental study with different 18650 high-power cells," *J. Energy Storage*, vol. 6, pp. 125–141, May 2016.

[64] L. E. Downie, L. J. Krause, J. C. Burns, L. D. Jensen, V. L. Chevrier, and J. R. Dahn, "In Situ detection of lithium plating on graphite electrodes by electrochemical calorimetry," *J. Electrochem. Soc.*, vol. 160, no. 4, pp. 588–594, 2013.

[65] P. Braun, J. Cho, J. Pikul, W. King, and H. Zhang, "High power rechargeable batteries," *Current Opinion Solid State Mater. Sci.*, vol. 16, pp. 186–198, 2012.

[66] M. Dubarry, M. Berecibar, A. Devie, D. Anseán, N. Omar, and I. Villarreal, "State of health battery estimator enabling degradation diagnosis: Model and algorithm description," *J. Power Sources*, vol. 360, pp. 59–69, 2017.

[67] L. Tan, L. Zhang, Q. Sun, M. Shen, Q. Qu, and H. Zheng, "Capacity loss induced by lithium deposition at graphite anode for LiFePO4/graphite cell cycling at different temperatures," *Electrochim. Acta*, vol. 111, pp. 802–808, Nov. 2013.

[68] E. Sarasketa-Zabala, F. Aguesse, I. Villarreal, L. M. Rodriguez-Martinez, C. M. López, and P. Kubiak, "Understanding lithium inventory loss and sudden performance fade in cylindrical cells during cycling with deep-discharge steps," *J. Phys. Chem. C*, vol. 119, no. 2, pp. 896–906, 2015.

[69] M. Dubarry, N. Qin, and P. Brooker, "Calendar aging of commercial Li-ion cells of different chemistries—A review," in *Current Opinion in Electrochemistry*, vol. 9. Elsevier, pp. 106–113, 2018.

[70] J. Groot, M. Swierczynski, A. I. Stan, and S. K. Kær, "On the complex ageing characteristics of high-power LiFePO4/graphite battery cells cycled with high charge and discharge currents," *J. Power Sources*, vol. 286, pp. 475–487, Jul. 2015.

[71] M. Petzl, M. Kasper, and M. A. Danzer, "Lithium plating in a commercial lithium-ion battery—A low-temperature aging study," *J. Power Sources*, vol. 275, pp. 799–807, Feb. 2015.

[72] M. C. Smart and B. V. Ratnakumar, "Effects of electrolyte composition on lithium plating in lithium-ion cells," *J. Electrochem. Soc.*, vol. 158, no. 4, pp. A379–A389, 2011.

[73] M. Petzl and M. A. Danzer, "Nondestructive detection, characterization, and quantification of lithium plating in commercial lithium-ion batteries," *J. Power Sources*, vol. 254, pp. 80–87, May 2014.

[74] S. M. Rezvanizaniani, Z. Liu, Y. Chen, and J. Lee, "Review and recent advances in battery health monitoring and prognostics technologies for electric vehicle (EV) safety and mobility," *J. Power Sources*, vol. 256, pp. 110–124, Jun. 2014.

[75] X. Xu, Z. Li, and N. Chen, "A hierarchical model for lithium-ion battery degradation prediction," *IEEE Trans. Rel.*, vol. 65, no. 1, pp. 310–325, Mar. 2016.

[76] L. Sánchez *et al.*, "Assessing the health of LiFePO4 traction batteries through monotonic echo state networks," *Sensors*, vol. 18, no. 2, p. 9, Dec. 2017.

David Anseán received the M.Eng. degree from the University of Granada, Granada, Spain, in 2007, and the Ph.D. degree (with honors) from the University of Oviedo, Spain, in 2015, both in electronics engineering.

He gained international experience (Basingstoke, U.K., and Berkeley, CA, USA) in technological companies after receiving the M.Eng. degree. After receiving the Ph.D. degree, he joined the University of Hawaii, Hawaii, USA, as a Postdoctoral Fellow, to work on advanced diagnosis and prognosis techniques on lithium-ion batteries. He joined the University of Oviedo, Spain, as an Assistant Professor in 2016. He is the Instructor of undergraduate and graduate courses including power electronics, digital integrated circuits, and embedded systems. His research interests include lithium-ion battery degradation mechanisms analysis via non-invasive methods, battery testing, and characterization, and design of battery fast charging. Q8

As a doctoral student, Dr. Anseán was the recipient of a research fellowship stay at the Electrochemical Power Systems Laboratory, at the University of Hawaii, USA. In 2018, he was the recipient of a Visiting Scholar Research Fellowship at the Institute for Power Electronics and Electrical Drives (ISEA) at RWTH Aachen University, Germany.

Víctor Manuel García Fernández received the Ph.D. degree in chemistry from the University of Oviedo, Spain.

Currently, he is an Associate Professor in the area of physical chemistry, where he teaches applied electrochemistry, centering around quantitative description of thermodynamic and kinetics phenomena in batteries and electrochemical corrosion cells. He is a member of the Battery Research Laboratory, where he collaborates in the electrochemical and thermal characterization, and modeling of Li-ion cells, and in the application of techniques, such as incremental capacity, peak area, and electrochemical impedance spectroscopy to quantify the effects of aging on materials.

Manuela González received the M.Sc. and the Ph.D. degrees in electrical engineering from the University of Oviedo, Spain, in 1992 and 1998, respectively.

She is the Founder and Head of the "Battery Research Laboratory" in the Electrical Engineering Department of University of Oviedo, a multidisciplinary team that focuses its research on the electrical and chemical characterization of batteries, the design of efficient fast-charging and management methods. She has collaborated in more than 25 R&D battery-related projects, combining the research with the transference of results to companies. With over 20 years of experience in the field of batteries, her research interests include novel Li-ion technologies for transportation and energy storage systems applications, including the development of advanced state-of-health estimation methods.

Cecilio Blanco received the M.Sc. and Ph.D. degrees in electrical engineering from the University of Oviedo, Spain, in 1989 and 1996, respectively.

Since 1989, he has been with the Department of Electrical and Electronic Engineering, University of Oviedo, where he is currently an Associate Professor and the Head of the Instrumentation and Energy Storage Systems Group. His research interests include electronic instrumentation systems, battery characterization, and modeling.

Juan Carlos Viera received the Ph.D. degree from the University of Oviedo, Spain, in 2003.

Currently, he is an Associate Professor with the Electrical and Electronics Engineering Department of the University of Oviedo. He has over 20 years of battery researching experience. He leads and collaborates with several projects, especially in the field of electric vehicles and battery energy storage systems. His research interests include energy storage systems, new advanced battery technologies, and battery management systems, focusing on the design of battery test benches, and electrical and chemical characterization under standard/stressful conditions.

Yoana Fernández Pulido received the B.Sc. degree in Chemistry from the University of Oviedo, Spain, in 2010, and the M.Sc. degree in Science and Chemistry Technology from The National Distance Education University (UNED), Madrid, Spain, in 2013. She is currently working toward the Ph.D. degree at the Battery Research Laboratory at University of Oviedo.

She worked as a Researcher with the Chemistry faculty at the University of Oviedo until 2015.

Luciano Sánchez received the M.Sc. and Ph.D. degrees in electronic engineering, from the University of Oviedo, Spain, in 1991 and 1994, respectively.

He has led 6 research projects supported by the Spanish government, 4 regional projects, and 16 privately funded research contracts. He was an external consultant for Electromateriales KLK (1991–1995), Saint-Gobain Cristalería (2000–2002), HC Energía (2003–2005), ITVASA (2005–2008), Indra Sistemas S.A. (2010–2011), Treelogic (2012–2014), GAMESA Corp (2014), Rolls-Royce Deutschland (2017), and RENFE (2018). He was also Visiting Scholar with UC Berkeley, Berkeley, CA, USA (1995), and GE Global Research (1996). He is a Professor with the Computer Science Department at the University of Oviedo, Spain. He is Head of the Research Group Metrology and Models, and Founding Partner of the spinoff of the research group IDALIA S.L. He has authored more than 70 international journals and more than 130 conference papers and book chapters, obtaining more than 4500 citations. His research interests include the theoretical study of algorithms for mathematical modeling and intelligent data analysis, and the application of these techniques to practical problems of industrial modeling, signal processing, and dimensional metrology, with special interest in the study of low-quality data.

Dr. Sánchez was the recipient of the IEEE Outstanding Paper Award in the 2013 IEEE International Conference on Fuzzy Systems (Hyderabad, India) and the 2013 Rolls-Royce Deutschland Engineering Innovationspreis (Berlin, Germany).

GENERAL INSTRUCTIONS

- **Authors: Please check ALL author names for correct spelling, abbreviations, and order of first and last name in the byline, affiliation footnote, and bios.**
- **Authors: We cannot accept new source files as corrections for your paper. If possible, please annotate the PDF proof we have sent you with your corrections and upload it via the Author Gateway. Alternatively, you may send us your corrections in list format. You may also upload revised graphics via the Author Gateway.**
- **Authors: Please note that once you click "approve with no changes," the proofing process is now complete and your paper will be sent for final publication and printing. Once your paper is posted on Xplore, it is considered final and the article of record. No further changes will be allowed at this point so please ensure scrutiny of your final proof.**
- **Authors: Unless invited or otherwise informed, a mandatory Excessive Paper Length charges will be incurred if your paper is over the page limit set by the society in the Information for Authors. If you have any questions regarding overlength page charges, need an invoice, or have any other billing questions, please contact reprints@ieee.org as they handle these billing requests.**

QUERIES

Q1. Author: Please confirm or add details for any funding or financial support for the research of this article.
Q2. Author: Please provide the significance of bold entities given in Table I.
Q3. Author: Please check the edits made to the sentence "However, analyzing IC and PA..." for correctness.
Q4. Author: Please provide publisher location for Refs. [16], [49], and [69].
Q5. Author: Please provide page range for Ref. [48].
Q6. Author: Please provide department for Ref. [50].
Q7. Author: Please check whether Ref. [57] is okay as set.
Q8. Author: Please check the edits made to the sentence "He gained international..." for correctness.

Lithium-Ion Battery Degradation Indicators Via Incremental Capacity Analysis

David Anseán, Víctor Manuel García, Manuela González, Cecilio Blanco-Viejo, Juan Carlos Viera, Yoana Fernández Pulido, and Luciano Sánchez

***Abstract*—Lithium-ion battery (LIB) degradation originates from complex mechanisms, usually interacting simultaneously in various degrees of intensity. Due to its complexity, to date, identifying battery aging mechanisms remains challenging. Recent improvements in battery degradation identification have been developed, including validated, *in situ* incremental capacity (IC) and peak area (PA) analysis. Due to their *in situ* and non-destructive nature, IC and PA implementation is feasible in on-board battery management systems (BMSs). Despite their advantages, the understanding and applicability of IC and PA techniques is not straightforward, as it requires both electrochemical and material science backgrounds. However, BMS design teams are mainly integrated by electrical engineers and may not include battery scientists. Aiming to bridge gaps in knowledge between electrical engineering and battery science toward battery degradation identification, here we present a systematic approach consisting in a set of lookup tables generated from IC and PA techniques. The lookup tables provide a simple, yet reliable, tool for the evaluation of LIB degradation modes. Various real-life examples of cell degradation are also presented to illustrate and validate the use of the proposed approach. This study exemplifies the use of lookup tables providing a simple, fast, and accurate automated estimation of LIB degradation modes to be implemented in BMSs.**

***Index Terms*—Battery degradation modes, incremental capacity (IC) analysis, lithium-ion battery (LIB), lookup tables.**

I. Introduction

LITHIUM-ION batteries (LIBs) have become ubiquitous in our society, particularly for its use in consumer electronic devices, such as cell phones, laptops, or tablets [1], [2]. Similarly, in virtue of continuous improvements in battery research, LIBs have also become the power source of choice for sustainable transportation, e.g., electric vehicles (EVs) and hybrid vehicles (HEVs) [3]–[6]. Recently, LIBs are gaining momentum in applications of massive electrical energy storage, i.e., battery energy storage systems (BESS) [7]–[10]. In view of these facts, LIBs are playing a fundamental role globally, both in industrial and commercial applications.

Despite its steady progress, LIB systems still face issues to be addressed, mainly related to degradation and performance [11], and management methods [12], [13]. Indeed, the study of aging and failure mechanisms has developed at a much slower pace than LIB performance [14]. Battery degradation presents a major concern in long-term, reliable applications, including EVs, BESS, and aerospace systems, where long cycle life under demanding duty schemes is required. Similarly, it is equally important to measure and estimate the functional status of the battery and protect it from hazardous conditions. Indeed, different degradation phenomena in LIBs lead to different aging patterns and failure modes [15]. All those critical parameters are to be assessed in the BMS. Therefore, to improve the overall system's capabilities, it becomes essential to both understand and identify the LIB degradation phenomena and integrate these features in BMSs.

To understand and evaluate cell degradation phenomena, numerous techniques—including *in situ* and *postmortem*—have been developed [16]–[18]. Among *in situ* techniques that are feasible in BMS applications, IC and PA are recognized as some of the most advanced, non-invasive techniques to identify LIB degradation modes [19]–[22]. Despite the established advantages of using IC and PA to monitor cell degradation, these analyses usually appear tedious at first, particularly for those unfamiliar with these techniques.

The main disciplines that technically contribute to the assessment of cell degradation (i.e., Material Science–Electrochemistry and Electrical Engineering–Computer Science), do not often interact. An optimal design of LIB systems shall involve both scientists and engineer's collaboration at its core. In addition, a fundamental understanding of each other's background shall be required. The approach behind this concept is shown in Fig. 1, where we aim to illustrate the importance of linking Battery Science and Battery Engineering, to design state-of-the-art, reliable, and efficient battery systems.

Herein, we present a framework to systematically analyze cell degradation via IC and PA via lookup tables. Lookup tables are commonly used in computer science to save processing time,

Manuscript received August 2, 2018; revised October 29, 2018; accepted December 19, 2018. Paper 2018-PEDCC-0553.R1 presented at the 2017 IEEE International Conference on Environment and Electrical Engineering and 2017 IEEE Industrial and Commercial Power Systems Europe, Milan, Italy, Jun. 6–9, and approved for publication in the IEEE Transactions on Industry Applications by the Power Electronic Devices and Components Committee of the IEEE Industry Applications Society. This work was supported in part by the Science and Innovation Ministry and in part by FEDER, under Projects DPI2013-046541-R, TIN2014-56967-R, TEC2016-80700-R (AEI/FEDER, UE), and TIN2017-84804-R. *(Corresponding author: David Anseán.)*

D. Anseán, M. González, C. Blanco-Viejo, J. C. Viera, and Y. F. Pulido are with the Electrical Engineering Department, University of Oviedo, Gijón 33203, Spain (e-mail: anseandavid@uniovi.es; mgonzalez@uniovi.es; cecilio@uniovi.es; viera@uniovi.es; fernandezyoana@uniovi.es).

V. M. García is with the Physical and Analytical Chemistry Department, University of Oviedo, Gijón 33203, Spain (e-mail: victorg@uniovi.es).

L. Sánchez is with the Computer Science Department, University of Oviedo, Gijón 33203, Spain (e-mail: luciano@uniovi.es).

Color versions of one or more of the figures in this paper are available online at http://ieeexplore.ieee.org.

Digital Object Identifier 10.1109/TIA.2019.2891213

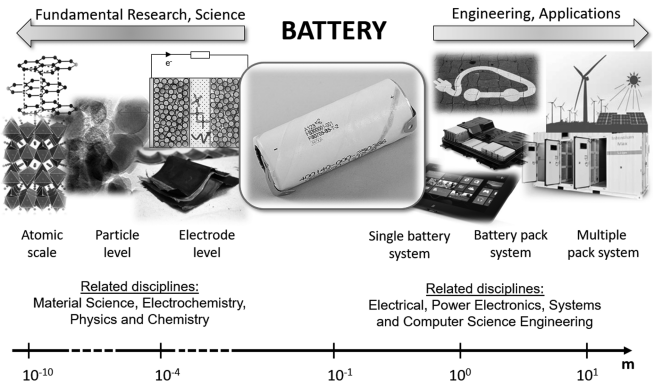

Fig. 1. General perspective of disciplines, background, and system levels that takes place in the design of lithium-ion battery systems.

although the approach is applied in different fields [23]–[25]. In this paper, the lookup tables present the main LIB degradation modes and their relation to IC and PA patterns. The lookup tables avoid extensive and non-straightforward electrochemical analyses, therefore facilitating LIB degradation identification for BMS integration.

We shall begin with a brief background of cell aging mechanisms and IC and PA analysis, then present the lookup tables, and conclude with examples of real LIB experiments, to illustrate the use and applicability of the framework using lookup tables. Due to space constrains, this paper is focused in one LIB cell technology, commonly used graphite‖lithium iron phosphate (GIC‖LFP). However, the high-level methodology presented here is valid for all intercalation LIB materials found in almost every commercial LIB system.

II. Theoretical Background—Cell Aging Mechanisms, Incremental Capacity (IC), and Peak Area (PA) Analysis

A. LIB Aging Mechanisms

Overall, LIBs degrade by capacity and power fade [14]. However, the underpinning phenomenon that originates LIB degradation involves more complex processes. These processes are originated from multiple degradation mechanisms, usually taking place simultaneously [11]. These degradation mechanisms are commonly identified as loss of lithium inventory (LLI), loss of active material (LAM), ohmic resistance increase (ORI), and lithium plating [11], [26], [27].

From the different cell degradation modes, LLI is generally the primary source, leading to direct capacity fade [26], [28]. LLI is a loss of usable Li ions, caused by parasitic reactions that are originated within the cell, and are mainly attributed to the continuous growth of the solid electrolyte interface (SEI) layer [29]. The LAM is related to structural and mechanical degradation of the electrodes [28]. Although LLI can take place alone [30], [31], LAM takes place simultaneously with LLI, as studies indicate [19], [32]–[35]. Recently, LAM has been experimentally demonstrated to have "silent" effects, i.e., degradation that is not exhibited in cell capacity fade [36]. This peculiar "silent" degradation can eventually trigger sudden appearances of rapid capacity loss, known as second degradation stages [26]. Overall, LAM can lead to both capacity and power fade. The ORI causes a shift of the voltage potential of the cell, therefore reducing its energy efficiency. ORI is generally referred as the degradation caused on the electrodes and electrolyte materials that directly result in an increase of the electronic and ionic resistance of a cell. ORI generally results from various sources of cell degradation, including LLI (SEI growth and destabilization [29]) and LAM (e.g., particle isolation, binder decomposition [11]). Lastly, lithium plating is considered as one of the most detrimental degradation modes in LIBs; it increases the rate of cell capacity fade, and may lead to safety issues due to dendrite growth that can internally short circuit the cell [37]. Metallic lithium is highly reactive, thus consuming usable Li ions (i.e., LLI) [34], and further increasing the rate of LLI [11], [36]. Similarly, lithium plating may block pores, isolate active particles and/or delaminate collector, leading to LAM [11], [38], [39]. In-depth analyses on LIB aging mechanisms can be found in reviews [11], [15], [37], [39]–[42], showing the relevance of these phenomena.

B. IC Analysis

The IC analysis identifies cell degradation mechanisms at electrode level. This information, contrary to less advanced, standard battery aging measurements (e.g., internal resistance and capacity fade evaluation), allows accurate battery diagnosis in a time-resolved manner. Another key advantage of IC is the ability to enable battery prognosis, thanks to the identification of the cell aging modes. Finally, a decisive BMS design condition is also accomplished, since the IC is implemented *in situ*. In all, due to these advantages, IC is recognized as a key technique to infer cell degradation, feasible in BMS applications.

Technically, the IC is an *in situ* electrochemical technique that detects the gradual changes in cell behavior, with great sensitivity, by studying the evolution with cycling of the resulting IC curves. The IC analyses are based on the original work by Thompson in 1979 [43], applied to material science research. It was later used in the 1990s by Dahn, to characterize carbon materials for LIB applications [44], and more recently by Dubarry and other groups [20], [21], [26], [45]–[48], to monitor cell degradation avoiding complex *postmortem* analyses.

Mathematically, the IC results from the ratio between an increment of capacity and a fixed voltage increment ($\mathrm{IC} = \Delta Q/\Delta V$). By tracking the increments of capacity associated with the voltage steps, the IC curve is generated. To illustrate the procedure, Fig. 2. is presented; the curve shows the evolution of cell voltage versus the state of charge. A fixed-voltage step (ΔV) yields different capacities (ΔQ_n), as cell voltage evolves. Applying $\mathrm{IC}_n = \Delta Q_n/\Delta V$ yields for this example $\mathrm{IC}_2 > \mathrm{IC}_1 > \mathrm{IC}_3 > \mathrm{IC}_4$. Hence, depending on the cell voltage profile, IC peaks with different intensities are formed. As expected from the mathematical expression, cell voltage plateaus result in large capacity increments (ΔQ_2), which yields large IC peaks. Conversely, abrupt cell voltage changes result in small capacity increments (ΔQ_4).

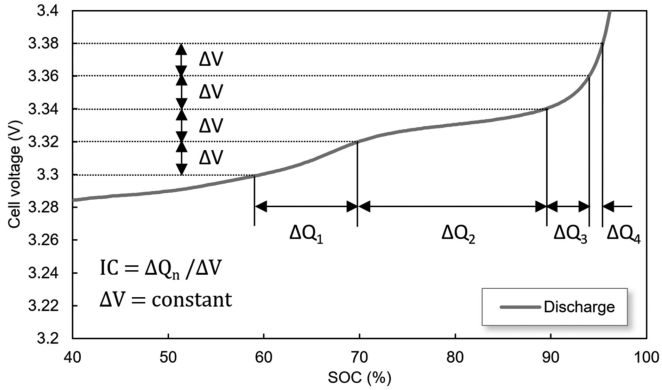

Fig. 2. Graphical representation of the IC values for a given SOC interval in a lithium-ion battery.

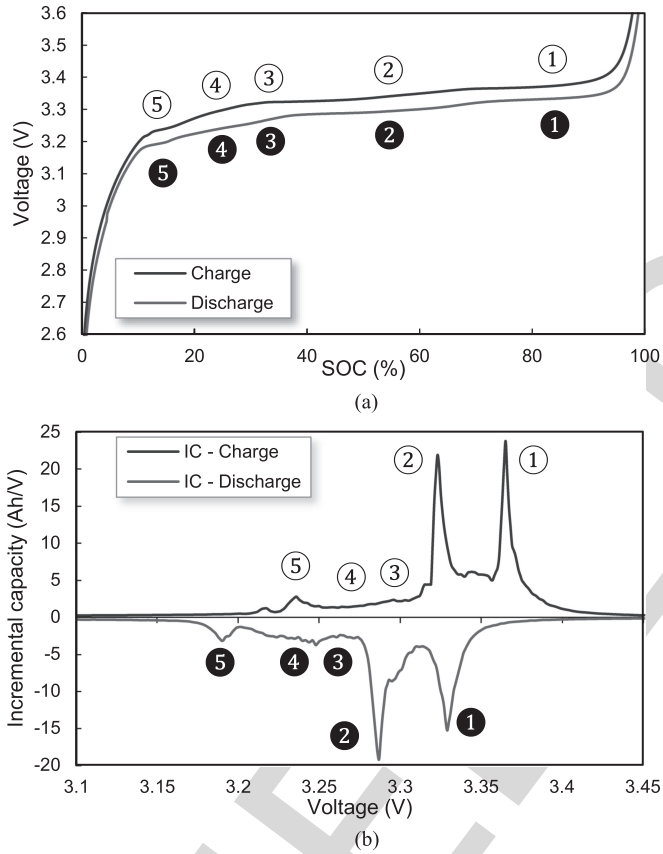

Fig. 3. (a) Charge (blue) and discharge (red) curves of a GIC‖LFP cell at C/25. (b) Shows the resulting IC curves.

To better illustrate IC, Fig. 3 is presented: Fig. 3(a) shows the charge/discharge curves of a commercial GIC‖LFP cell and Fig. 3(b) shows the resulting IC curves cycled at C/25.

The IC peaks are labeled as (①, ②, ③, ④, and ⑤) for charge, and (❶, ❷, ❸, ❹, and ❺) for discharge. Each IC peak is labeled according to the different electrochemical staging phenomena that take place in the cell [26]. Each IC peak is the result of the convolution of the electrochemical reactions in the active positive and negative electrode materials [49]. That is, the resulting IC peaks contain electrochemical signatures of both electrodes and exhibit a unique shape and intensity. Therefore,

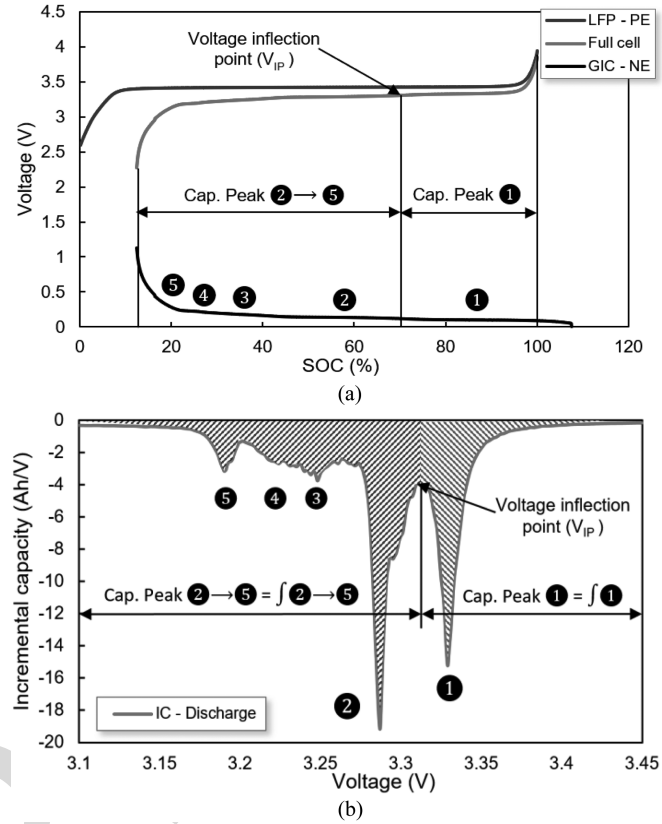

Fig. 4. (a) Discharge curve of a GIC‖LFP cell at C/25, showing the individual electrodes (positive, blue, negative, black) and the resulting full cell curve (red). In (b), the schematic representation to obtain the PA is presented.

tracking the evolution of IC peak's shape and position as the cell ages reveals key information on the cell electrochemical phenomena and electrode degradation mechanisms.

C. PA Analysis

PA is a technique derived from the IC, and quantifies the area associated with the phase transformations of a cell. These phase transformations correspond to the formation of solid solutions, and are detected from the IC inflection points [19], [45]. Hence, the PA yields the capacity underneath the IC peaks. This information is used to quantify the degree of degradation within a phase transformation of a LIB.

Fig. 4 presents the PA technique: Fig. 4(a) shows the voltage profile of a commercial GIC‖LFP cell (red curve). This voltage is obtained from the subtraction of the positive electrode (blue, LFP) minus the negative electrode (black, graphite). The PA is calculated from the capacity associated underneath the IC peaks [dashed area, see Fig. 4(b)], which correspond to various phase transformations.

For a better detection and quantification of the aging modes in this cell technology, it is recommended to separate the area underneath peak ❶ and the area associated to peaks ❷–❺. This is because the predominant aging mode (i.e., LLI) primarily affects peak ❶ [26], whereas another common degradation mode (i.e., LAM on the NE) affects peaks ❷–❺.

To calculate the area of a peak, i.e., ∫❶, the IC curve [see Fig. 4(b)] is generated. Then, the cell voltage inflection point (V_{IP}) between peak ❶ and ❷ is detected. The inflection point is evaluated versus the cell state of charge [see Fig. 4(a)], yielding ∫❶. Subtracting the full cell capacity minus ∫❶ yields the PA of ❷–❺, i.e., ∫❷–❺. The PA distribution can be directly given in Ah, or in terms of percentage of the total cell capacity (i.e., relative to the SOC).

The evolution of the PA distribution changes as the cell ages according to IC. Hence, tracking the evolution of the PA allows for an *in situ* evaluation of degradation modes from a quantitative perspective (i.e., in Ah), complementing advanced IC diagnosis.

D. Identification of Cell Degradation Via IC and PA Analyses

Degradation mechanisms in LIBs result from various aging modes: LLI, LAM, ORI, and lithium plating. Furthermore, LAM is divided into four degradation modes on the negative electrode (i.e., $\mathrm{LAM_{NE}}$) and/or in the positive electrode (i.e., $\mathrm{LAM_{PE}}$), either on delithiated (de) or lithiated (li) state, giving a total of four aging modes (i.e., $\mathrm{LAM_{deNE}}$, $\mathrm{LAM_{dePE}}$, $\mathrm{LAM_{liNE}}$, and $\mathrm{LAM_{liPE}}$) [26]. Each aging mode affects both the IC and PA curves in a unique manner. Hence, the analysis of each aging mode is required to construct the lookup tables.

As an example to show lookup table construction from IC and PA curves, this subsection presents the most common aging mode (i.e., LLI). The approach presented here is applied to all degradation mechanisms. A comprehensive analysis of each of the aging modes is out of the scope of this paper, and can be found elsewhere [26], [50]. In particular, Birkl *et al*. [28] have made significant progress in this area, providing an experimental proof of degradation modes.

LLI: In LIBs, LLI is described from an electrode perspective as a "slippage," as defined in [26], [51], and [52]. This slippage is described as the mechanisms of which the NE continues to move or shifts toward higher SOCs, while the capacity decreases gradually [53]. The slippage has been experimentally observed and measured in previous works [28], [31], [54], [55], and has also been incorporated in simulation for LIB diagnosis and prognosis analyses [22], [26], [56]. The slippage causes a reduction of IC peak ❶, and its area underneath (i.e., ∫❶), as indicated by arrow ❶ (see Fig. 5). This is because the graphite stage ❶ has been shifted outside the voltage window of the full cell (see Fig. 5, inset figure). Only upon large peak ❶ reduction (i.e., when peak ❶ is extinct), peak ❷ begins to reduce. LLI also causes a slight shift of peak ❺ upon cycling toward high cell potentials. However, its intensity (i.e., ∫❺) is not reduced. Peaks ❸ and ❹ are barely altered by the effect of LLI. Finally, peak ❶ and ❷ voltage inflection point remains constant, although its height is reduced.

The effects of LLI on the PA are shown in Fig. 6(a). As observed, constant rate LLI induces a linear capacity fade of ∫❶, reaching a point where all its capacity is lost (for this example, at cycle 1250). In contrast, ∫❷–❺ evolution remains unaffected, until ∫❶ is extinct. From that point (i.e., cycle 1250), ∫❷–❺ begins to lose capacity linearly. The normalized capacity evolution under constant rate LLI induces a linear capacity loss throughout cycling [see Fig. 6(b)].

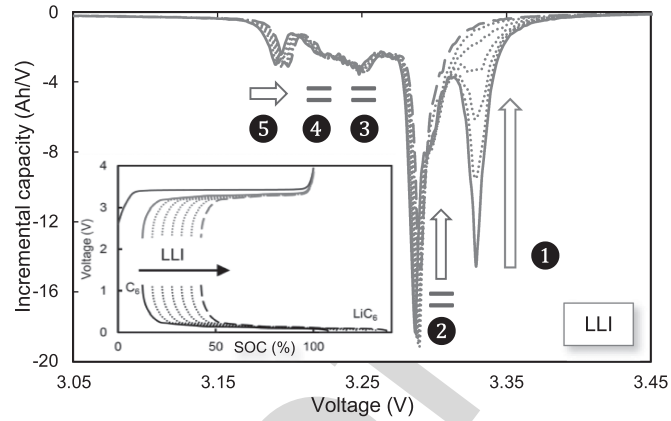

Fig. 5. IC signatures of LLI evolution from beginning (solid line) to end of cycling (dashed). Inset figure shows the NE slippage effect.

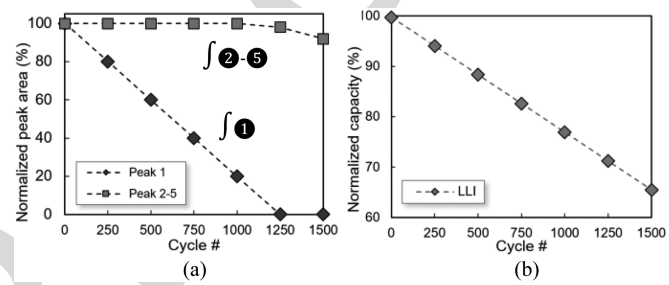

Fig. 6. (a) Normalized PA evolution under LLI for peak 1 (diamond) and peak 2–5 (squared). (b) Capacity fade evolution caused by the effect of LLI alone.

In brief, LLI mainly affects IC peak ❶ and PA ∫❶. Only under massive cell degradation, ∫❷–❺ is reduced. Peak ❺ can be used as a succinct indicator, tracking its slippage to higher cell voltages. In total, to identify LLI in a GIC‖LFP cell, one should verify peak ❶ and ∫❶ reduction, peak ❺ slippage, while peaks ∫❷–❺ remain unaffected.

III. Experimental

In this paper, we carry out both computer simulations and experimental cell cycle testing. Computer simulations were carried out using the '*alawa* toolbox, developed at the University of Hawaii [26], [57]. Simulations were used to obtain the IC and PA patterns of cell degradation mechanisms (LLI, LAM, ORI, and lithium plating). The model for the computer simulations was constructed using harvested real cell data, as described in [45]. This allows higher accuracy to generate the degradation patterns that are used to construct the lookup tables. Computer simulations were also used to create specific cell evolution patterns.

The experimental procedures were carried out on commercial GIC‖LFP batteries (2.3 Ah), using an Arbint BT-2000 battery tester. For the experiments, a Memmert environmental chamber was used to maintain the cells at 23 °C throughout testing.

To illustrate the usage of the lookup tables, three representative examples of real-life cell capacity evolution patterns are analyzed in this paper. This shall exemplify deciphering cell ag-

TABLE I
LOOKUP TABLE OF MAIN AGING MODES PARTICULARIZED FOR GIC‖LFP CELL DURING DISCHARGE. NOTICE THAT ARROW (↑) INDICATES IC PEAK REDUCTION MAIN FEATURES OF CELL DEGRADATION Q2

Aging modes	Incremental Capacity (peak number)						Peak Area		Cell external and internal constructive parameters				
	❶	❷	❸	❹	❺	⓪	∫❶	∫❷-❺	Capacity fade	Loading ratio	Offset	"Silent"	Risk of plating
LLI	↑	=/↑	=	=	→	=	Decreases/ Depleted	Unchanged/ Decreases	Increases	Unchanged	Increases	No	No
LAM_{deNE}	↓↑	↑	↑	↑	↖	=/=,↓	Increases/ Decreases	Decreases	Unchanged / NL increase or unchanged	Decreases	Unchanged	Yes	Yes
LAM_{liNE}	↑	↑	↑	↑	↗	=	Decreases	Decreases	Increases	Decreases	Increases	No	No
LAM_{dePE}	=/↙	=/↑	=/↑	=/↑	↑	=	Not affected	Unchanged/ NL decreases	Unchanged/ NL increase	Increases	Decreases	Yes	No
LAM_{liPE}	↑	=/↑	=	=	=	=	Decreases/ Depleted	Unchanged/ Decreases	Increases	Increases	Not affected	No	No
ORI	←	←	←	←	←	=	Decreases	Not affected	Increases	Unchanged	Unchanged	No	Yes

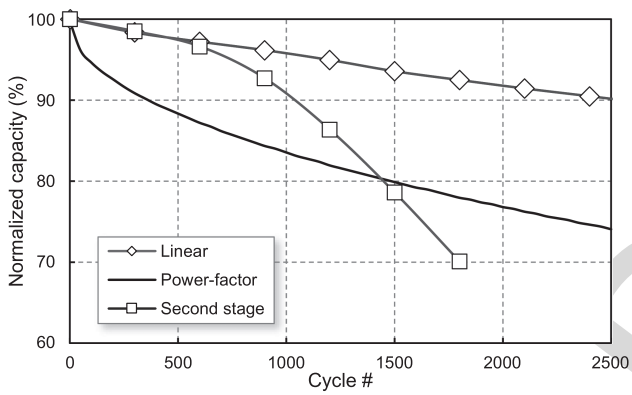

Fig. 7. Normalized capacity versus cycle number for the three most representative cell capacity evolution patterns.

ing modes under realistic scenarios. According to the literature, the most common capacity fade patterns are linear degradation [58]–[60], power-factor degradation [7], [27], [61], and non-linear, second-stage degradation [36], [62], [63].

Fig. 7 shows the three capacity evolution patterns used in this paper. Linear degradation pattern was obtained by continuous constant current cycling, as described in [45]. Power-factor degradation pattern was obtained via '*alawa* toolbox computer simulations, whereas the non-linear, second-stage degradation pattern was obtained by applying dynamic stress cycling, as described in [36]. We shall remark that capacity evolution patterns can give insights on the underlying aging mechanisms, but are not conclusive, since factors, such as temperature, cycling rate, cycling scheme, and/or cell cutoff voltage, modify the rate and shape of the capacity loss trend [36], [38], [41], [55], [63], [64]. Therefore, detailed analyses are to be carried out to decipher the aging modes, regardless of how those trends could be formed.

IV. RESULTS AND DISCUSSION

This section presents the lookup tables and discusses its usage for the three realistic capacity evolution patterns. In brief, each aging mode produces a specific IC and PA signature evolution as the cell ages. However, some aging modes may generate similar IC signatures, complicating its identification. Therefore, it is important to summarize and facilitate the IC and PA evolution for every aging mode, acting individually. These tendencies and features are summarized in the lookup table. As the lookup table is presented, the approach to analyze cell degradation gets simplified: One shall compare the experimental IC and PA results with those generated in the lookup tables, and proceed to evaluate these similarities. The identified change(s) shall correspond to the acting aging mode(s).

A. Lookup Table: IC, PA, and Cell Parameters

Table I presents the lookup table for GIC‖LFP cell technology. The table presents the aging modes (left column), and their effect on IC, PA, and cell external and internal constructive parameters (upper rows) during discharge.

The description of the symbols in the lookup table is as follows: (↑) indicates IC peak reduction and (↓) indicates IC peak increase. The horizontal arrows indicate a voltage shift of the peaks; (→) indicates higher cell voltages, whereas (←) indicates the opposite.

The equal symbol (=) indicates no change in IC patterns. The slash symbol (/) indicates a second degradation stage, i.e., an abrupt change in the capacity evolution pattern [26], [36]. During second degradation stages, the font type is set to red color. The rest of the table is self-described, except "NL" which stands for "non-linear."

Cell external and internal constructive parameter patterns are also described to gain in-depth analysis of the outcomes of the aging modes. External parameters are referred to those that can be directly measured (e.g., capacity fade), whereas internal parameters cannot be directly measured by standard procedures (e.g., cell architecture parameters) [26], [65].

Capacity fade describes the effects that a particular aging mode induces on capacity evolution. The loading ratio (LR) and offset (OFS) describe the stoichiometric cell construction. The LR is the ratio between the capacity contained in the negative and positive electrode (Q_{NE} and Q_{PE}), i.e., LR $= Q_{\mathrm{NE}}/_{\mathrm{PE}}$, as described in [26]. The OFS corresponds to the slippage of the NE over the PE, as previously commented. The table also presents whether the aging mode effect remains "silent" dur-

ing its first degradation stage, therefore indicating why there is no discernible loss of capacity [45]. Finally, the table also includes whether the aging modes can lead to direct lithium plating appearance: Peak ⓪ appearance and growth indicates thermodynamic lithium plating occurrence [36], [66].

In total, the use of the cell constructive parameters is critical for advanced diagnosis and prognosis analyses. In addition, since internal patterns cannot be directly measured, the use of the provided lookup table becomes instrumental. Next sections present further discussion and analyses of these parameters.

B. Use of the Lookup Tables in Real-Life Experiments

Here we illustrate the use of lookup tables to decipher cell aging modes, from real-life experiments. One of the implicit advantages of using lookup tables is their systematic nature; hence, an approach based on various steps can be generated. This approach is based on comparing experimental IC and PA curves versus the lookup tables.

We derive this analysis following the step-by-step process derived from experimental results demonstrated in previous works [19], [28], [36], [45].

1) Generate experimental IC and PA figures.
2) Number all IC peaks (i.e., ❶ to ❺) in the figures.
3) Indicate each IC peak with arrows: Direction, length, and intensity.
4) Analyze peak ❶: Reduction most likely indicates LLI, and to a much lesser degree $\mathrm{LAM_{PE}}$. Initial peak ❶ increase, or initial steady evolution indicates adding effect of $\mathrm{LAM_{deNE}}$.
5) Analyze peaks ❷–❺: Reduction indicates $\mathrm{LAM_{NE}}$, a highly likely scenario. No changes indicate LLI (highly likely) and/or $\mathrm{LAM_{PE}}$ (highly unlikely).
6) Analyze ∫❶ evolution: A reduction equal to the cell capacity fade indicates solely effect of LLI. Initial increase or steady evolution indicates $\mathrm{LAM_{deNE}}$. Reduction indicates $\mathrm{LAM_{liPE}}$ (highly unlikely).
7) Analyze ∫❷–❺ evolution: No changes indicate solely effect of LLI and/or $\mathrm{LAM_{PE}}$ (highly unlikely). Reduction indicates $\mathrm{LAM_{NE}}$.
8) Fine tuning via peak ❺ analysis: Shifting to the right without reduction indicates solely LLI; less intense shifting and reduction, indicates LLI+$\mathrm{LAM_{deNE}}$; intense shifting and reduction, indicates LLI+$\mathrm{LAM_{liNE}}$; $\mathrm{LAM_{PE}}$ affecting peak ❺ is highly unlikely.
9) Other scenarios: ⓪ peak appearance. This peak is associated to $\mathrm{LAM_{deNE}}$ and is related to thermodynamic lithium plating occurrence.

Following the step-by-step process should resolve cell aging modes identification. Further analyses based on literature studies are generally required for improved accuracy for aging mode identification; for example, LAM in the PE for LFP systems is very unlikely, as reported in postmortem analyses [35], [55], [67], [68].

1) Linear Degradation: Fig. 8 shows the IC and PA at C/25 obtained from the cell tested under constant current scheme

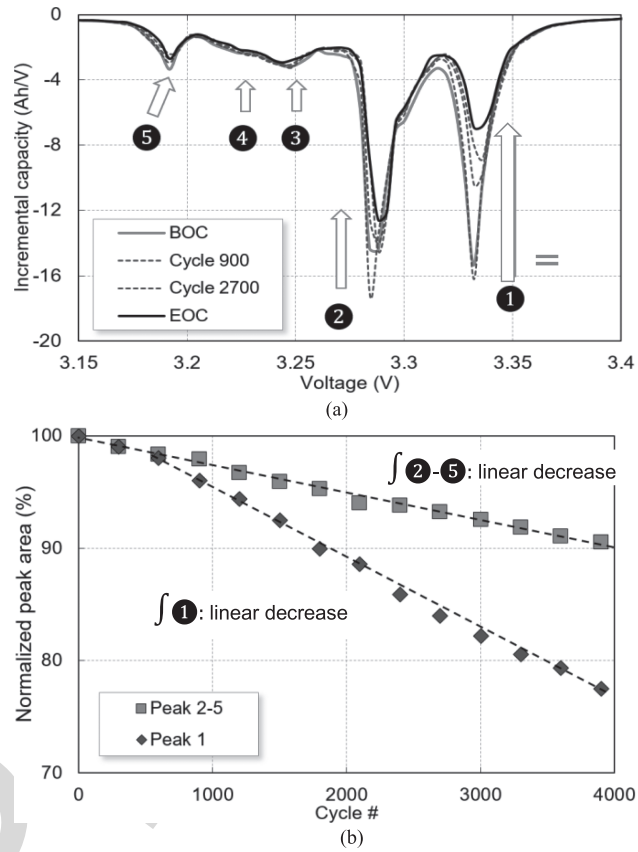

Fig. 8. Linear degradation pattern, and its resulting (a) IC and (b) PA curves.

[45]. The first steps (1–3) are to indicate and label all peaks, as shown in Fig. 8. Then, analyze peak ❶ and ❷–❺, following steps 4 and 5. We deduce that LLI and $\mathrm{LAM_{NE}}$ can be the main aging modes: Peak ❶ reduction accompanied with peak ❷–❺ proportional reduction. From steps 6 and 7, we further corroborate the suggestions: ∫❶ reduction together with ∫❷–❺ linear decrease also indicates LLI+$\mathrm{LAM_{NE}}$.

We now proceed to carry out fine tuning analyses: This shall allow us to separate the aging mode acting on the NE (i.e., $\mathrm{LAM_{deNE}}$ or $\mathrm{LAM_{liNE}}$). The main sensors are peak ❶ and peak ❺. The slight shift of peak ❺ counteracts the shift and reduction that $\mathrm{LAM_{deNE}}$ would produce (see Table I). In addition, peak ❶ reduction does not begin abruptly [see equal symbol in peak ❶ IC curve, see Fig. 8(a)], a fact that also matches with $\mathrm{LAM_{deNE}}$ signature.

The above-mentioned reasoning indicates that aging on the studied cell is caused by LLI (significant reduction of peak ❶), accompanied by the effect of $\mathrm{LAM_{deNE}}$ (reduction of peaks ❷–❺ and slight reduction of peak 1). In addition, due to the larger effects of LLI, we also conclude that aging mode LLI is more prominent than $\mathrm{LAM_{deNE}}$. These results are in agreement with the literature [19], [45].

2) Power Factor Degradation: Fig. 9 shows the IC and PA at C/25, obtained from the cell exhibiting power factor capacity fade, labeling and indicating IC peaks (steps 1–3). According to procedure steps (4–8), this particular example of cell aged under power factor degradation is aged from LLI alone: Only peak ❶

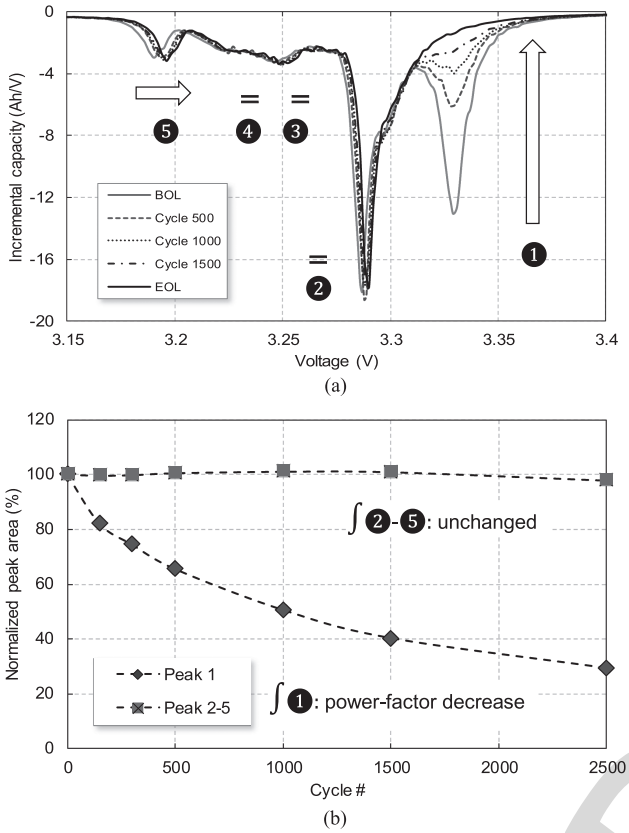

Fig. 9. Power factor degradation pattern, and (a) IC and (b) PA curves.

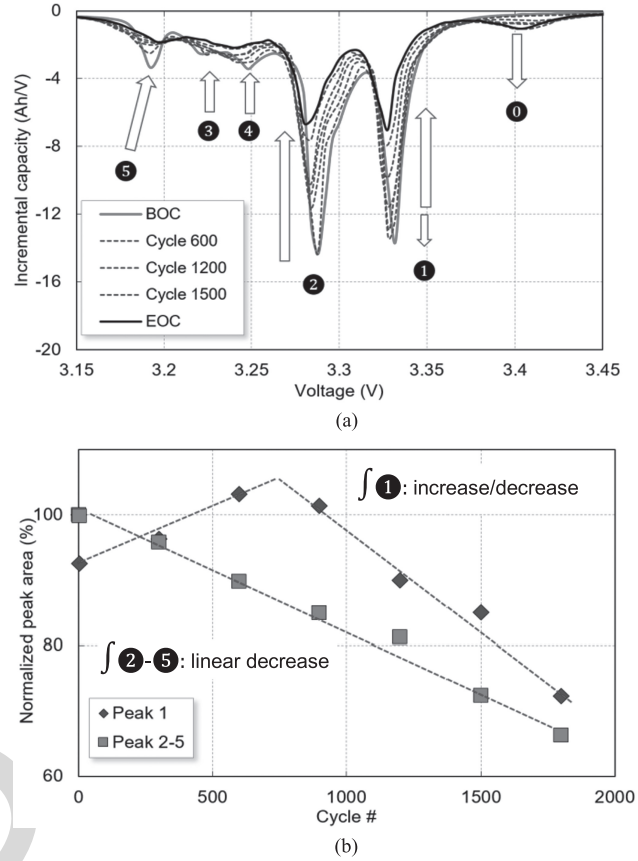

Fig. 10. Dynamic stress cycling, and its resulting (a) IC and (b) PA curves.

is reduced, ❷–❺ peak remains unchanged through cycling, and peak ❺ is shifted significantly toward higher cell voltage, but not reduced (i.e., ∫❺ remains constant).

This type of degradation pattern is generally found (but not exclusive to) in calendar-aged systems [30], [69], systems exposed to high temperatures [70] or systems where the effects of calendar aging are more prominent than those of cycling [61]. Under those conditions, LLI is the major cell aging mode. We shall point out that power factor degradation may not be exclusively caused by LLI, as studies shown [71].

3) Non-linear, Second-Stage Degradation: Fig. 10 shows the IC and PA at C/25 obtained from the cell tested under dynamic stress cycling. In this particular case, degradation seems very complicated at first; IC peaks shifting, reducing, increasing, and even appearing (see peak ⓪). Curiously, these signatures usually facilitate the analysis.

Analyzing steps 4–8 clearly indicates the effect of $\mathrm{LAM_{deNE}}$: Peak ❶ and ∫❶ initial increase, accompanied by peak ∫❷–❺ reduction can only lead to $\mathrm{LAM_{deNE}}$ (see Table I). In addition, LLI is acting to some extent, as peak ❶ and ∫❶ is also reduced, and peak ❺ is shifted to higher cell voltage. However, the most outstanding signature to evaluate cell degradation is the appearance of peak ⓪: This peak can only be derived by the effect of $\mathrm{LAM_{deNE}}$ (see step 9).

From this straightforward analysis, we conclude that the cell is under lithium plating occurrence due to peak ⓪ appearance. In addition, due to the larger effects associated with $\mathrm{LAM_{deNE}}$, we also conclude that aging mode $\mathrm{LAM_{deNE}}$ is more prominent than LLI. These results are in agreement with detailed studies [36], [72], [73].

4) External and Internal Constructive Parameter Analyses: The lookup table can be used to further evaluate cell constructive parameters (see Table I). Deciphering these parameters can lead to improvements in both BMS and cell design processes. Advanced information on lithium plating incubation and/or occurrence can be used in BMSs in various strategies: Modify and reduce the power requirements on the batteries, and/or set a warning state to replace the batteries. These strategies would avoid unnecessary risks of battery degradation or cell failure [36]. This approach also fails in the field of advanced battery prognosis [74], [75]. Tracking the evolution of the OFS and/or the LR can be applied to optimize the mass and area of electrode active materials within the cell for a specific application. The analyses of external and internal parameters illustrate the applicability of the lookup tables in linking both material science and electrical engineering disciplines under common analyses, with mutual objectives in cell and system design improvements.

For the linear degradation pattern, we deciphered LLI and $\mathrm{LAM_{deNE}}$ as the ongoing aging modes. According to Table I, their effects increase the OFS, while reducing LR. In addition, this aging mode combination could lead to lithium plating; however, since the effect of LLI is larger than that of $\mathrm{LAM_{deNE}}$,

this scenario remains unlikely [45]. Interestingly, the effects of $\mathrm{LAM_{deNE}}$ are silent, i.e., cannot be directly estimated from measuring capacity fade. However, analyzing IC and PA allows identifying the silent effect, both from a qualitative (IC), and quantitative (PA) perspective.

The non-linear, second-stage degradation was affected by $\mathrm{LAM_{deNE}}$ and LLI to an extent that induced lithium plating. Verifying the lookup table, the cell reduces its LR (caused by $\mathrm{LAM_{deNE}}$), increases OFS (caused by LLI), shows silent effects (caused by $\mathrm{LAM_{deNE}}$), and is under lithium plating occurrence due to large $\mathrm{LAM_{deNE}}$ effect.

The advantages of using the lookup tables for internal analyses are also exemplified when comparing both linear and non-linear degradation patterns: As observed, during the first 600 cycles (see Fig. 7), both cells show the same capacity fade pattern. Without a proper analysis of the IC and cell constructive parameters, patterns between cells appear identical. However, via IC and lookup table analyses, it is feasible to diagnose and prognose the non-linear, second degradation aging patterns.

5) System-Level Approach: From a system-level perspective, the implementation of the proposed strategy involves various design features to consider. To apply lookup table aging mode identification with highest accuracy, cycling under pseudo-thermodynamic conditions (i.e., C/25) yields optimal results. This slow cycling from reference performance tests (RPTs) can be carried out periodically (i.e., 6–12 mo, depending on the application). We shall point out that EVs or BESS battery packs are designed to last ten years or more of use, specifically BESS with longer life span. Hence, the RPT approach time frame is equivalent to regular maintenance services in other existing energy systems, or internal combustion engine vehicles. Therefore, this strategy shall not present major drawbacks for the overall operation of the system. For consumer electronics, the RPTs could be carried out more often (i.e., 2–4 mo), due to their lower life span. In addition to the high accuracy of C/25 tests, the IC curves obtained under kinetic cycling (i.e., C/2, 1C) can derive useful information to identify polarization resistances and kinetic degradation [20], [45]. These curves can be analyzed regularly, as kinetic cycling is generally found under normal system's usage (i.e., during charges), providing useful ongoing diagnosis information.

Advanced strategies are also being developed to reduce the impact of the maintenance services, aiming to carry out the analyses *in operando*. From a hardware perspective, large systems (i.e., BESS) could disconnect individual power modules to perform dedicated RPTs, without affecting the power capabilities or disconnecting the entire system. From a software perspective, onboard diagnosis using lookup tables with selected features of interest (FOI) of the IC curves can be implemented prior its deployment [66], reducing the need for full charge/discharge cycles. In addition to the above strategies, in future works, we aim to provide advanced approaches to decipher aging *in operando* using transformation models via soft sensors and fuzzy observers [76]. Similarly, future work shall be carried out for algorithm development for the selected BMS platform/architecture.

V. Conclusion

To date, LIB degradation analysis and aging mode identification presents a major concern in long-term, reliable LIB applications. As it becomes essential to integrate these features in state-of-the-art BMSs, this paper presents a systematic approach to identify LIB degradation modes, based on the validated, *in-situ*, IC electrochemical technique. The proposed methodology simplifies the relatively complex and non-straightforward IC analysis procedure, by using a set of inclusive lookup tables and a systematic step-by-step process. This approach is particularly interesting for electrical and system engineers who, despite being the main contributors in BMS design, do not often possess the background to perform this type of electrochemical analyses.

The methodology consists first on individually implementing all LIB degradation modes, analyze their corresponding IC and PA main features, and present them in the form of a lookup table. Then, the lookup table is complemented with a step-by-step procedure to provide a systematic path for LIB degradation identification. The final step consists of obtaining the IC and PA experimental results and following the designed methodology. This shall yield accurate results on LIB aging modes identification. To both validate and exemplify the use of the proposed methodology, we also presented three common, real-life capacity fade scenarios, and deciphered their aging modes.

In a broader perspective, this paper aims to provide a bridge in knowledge between battery science and electrical engineering, with the final objective of using these techniques in novel BMS. The methodology presented here, due to its systematic nature, can be implemented as an algorithm in a microprocessor-based system to be ultimately embedded in the BMS. The prospects of using this set of straightforward tools are attractive to improve BMS designs for battery diagnosis and prognosis.

This approach was applied to GIC‖LFP based batteries. However, the methodology is valid for all intercalation LIBs, which currently represent the vast majority of commercial LIBs. Future work shall focus on specific lookup tables and procedures for various battery chemistries (e.g., nickel manganese oxide, nickel–cobalt–aluminum, etc.). We anticipate that, although the proposed methodology remains unaltered, different IC peaks and FOI will emerge for each particular chemistry. We believe that the availability of the lookup tables in several battery chemistries would create interesting benefits and further discussions in the LIB research community.

References

[1] T. Reddy, *Linden's Handbook of Batteries*, 4th ed. New York, NY, USA: McGraw-Hill, 2011.

[2] G. E. Blomgren, "The development and future of lithium ion batteries," *J. Electrochem. Soc.*, vol. 164, no. 1, pp. A5019–A5025, Dec. 2017.

[3] D. Anseán, V. M. García, M. González, J. C. Viera, J. C. Antón, and C. Blanco, "Evaluation of $LiFePO_4$ batteries for electric vehicle applications," *IEEE Trans. Ind. Appl.*, vol. 51, no. 2, pp. 1855–1863, Mar./Apr. 2015.

[4] X. Gong, R. Xiong, and C. C. Mi, "Study of the characteristics of battery packs in electric vehicles with parallel-connected lithium-ion battery cells," *IEEE Trans. Ind. Appl.*, vol. 51, no. 2, pp. 1872–1879, Mar. 2015.

[5] M. Farhadi and O. Mohammed, "Energy storage technologies for high-power applications," *IEEE Trans. Ind. Appl.*, vol. 52, no. 3, pp. 1953–1961, May 2016.

[6] S. S. Williamson, A. K. Rathore, and F. Musavi, "Industrial electronics for electric transportation: Current state-of-the-art and future challenges," *IEEE Trans. Ind. Electron.*, vol. 62, no. 5, pp. 3021–3032, May 2015.

[7] D. I. Stroe, M. Swierczynski, A. I. Stan, R. Teodorescu, and S. J. Andreasen, "Accelerated lifetime testing methodology for lifetime estimation of lithium-ion batteries used in augmented wind power plants," *IEEE Trans. Ind. Appl.*, vol. 50, no. 6, pp. 4006–4017, Nov./Dec. 2014.

[8] D. I. Stroe, V. Knap, M. Swierczynski, A. I. Stroe, and R. Teodorescu, "Operation of a grid-connected lithium-ion battery energy storage system for primary frequency regulation: A battery lifetime perspective," *IEEE Trans. Ind. Appl.*, vol. 53, no. 1, pp. 430–438, Jan./Feb. 2017.

[9] B. Z. Ma, A. Pesaran, and V. Gevorgian, "Energy storage, renewable power generation, and the grid," *IEEE Electrific. Mag.*, vol. 3, no.3, pp. 30–40, Sep. 2015.

[10] B. Dunn, H. Kamath, and J. M. Tarascon, "Electrical energy storage for the grid: A battery of choices.," *Sci.*, vol. 334, no. 6058, pp. 928–935, Nov. 2011.

[11] J. Vetter *et al.*, "Ageing mechanisms in lithium-ion batteries," *J. Power Sources*, vol. 147, no. 1–2, pp. 269–281, Sep. 2005.

[12] W. Waag, C. Fleischer, and D. U. Sauer, "Critical review of the methods for monitoring of lithium-ion batteries in electric and hybrid vehicles," *J. Power Sources*, vol. 258, pp. 321–339, Jul. 2014.

[13] H. Rahimi-Eichi, U. Ojha, and M.-Y. Chow, "Battery management system—An overview of its application in the smart grid and electric vehicles," *IEEE Ind. Electron. Mag.*, vol. 7, no. 2, pp. 4–16, Jun. 2013.

[14] M. R. Palacín and A. De Guibert, "Batteries: Why do batteries fail?," *Sci.*, vol. 351, no. 6273, p. 1253292, Feb. 2016.

[15] C. Hendricks, N. Williard, S. Mathew, and M. Pecht, "A failure modes, mechanisms, and effects analysis (FMMEA) of lithium-ion batteries," *J. Power Sources*, vol. 297, pp. 113–120, Nov. 2015.

[16] M. Berecibar, I. Gandiaga, I. Villarreal, N. Omar, J. Van Mierlo, and P. Van Den Bossche, "Critical review of state of health estimation methods of Li-ion batteries for real applications," in *Renewable and Sustainable Energy Reviews*, vol. 56. Elsevier, pp. 572–587, 2016.

Q4 [17] P. P. R. M. L. Harks, F. M. Mulder, and P. H. L. Notten, "In situ methods for Li-ion battery research: A review of recent developments," *J. Power Sources*, vol. 288, pp. 92–105, Aug. 2015.

[18] B. Xu, A. Oudalov, A. Ulbig, G. Andersson, and D. S. Kirschen, "Modeling of lithium-ion battery degradation for cell life assessment," *IEEE Trans. Smart Grid*, vol. 9, no. 2, pp. 1131–1140, Mar. 2018.

[19] M. Dubarry, C. Truchot, and B. Y. Liaw, "Cell degradation in commercial $LiFePO_4$ cells with high-power and high-energy designs," *J. Power Sources*, vol. 258, pp. 408–419, Feb. 2014.

[20] M. Dubarry and B. Y. Liaw, "Identify capacity fading mechanism in a commercial $LiFePO_4$ cell," *J. Power Sources*, vol. 194, no. 1, pp. 541–549, Oct. 2009.

[21] M. Berecibar, M. Dubarry, I. Villarreal, N. Omar, and J. Van Mierlo, "Degradation mechanisms detection for HP and HE NMC cells based on incremental capacity curves," in *Proc. IEEE Veh. Power Propulsion Conf.*, pp. 1–5, Oct. 2016.

[22] X. Han, M. Ouyang, L. Lu, J. Li, Y. Zheng, and Z. Li, "A comparative study of commercial lithium ion battery cycle life in electrical vehicle: Aging mechanism identification," *J. Power Sources*, vol. 251, pp. 38–54, Apr. 2014.

[23] R. Xiong, H. He, F. Sun, and K. Zhao, "Evaluation on state of charge estimation of batteries with adaptive extended Kalman filter by experiment approach," *IEEE Trans. Veh. Technol.*, vol. 62, no. 1, pp. 108–117, Jan. 2013.

[24] T. Inoue, S. Miyazaki, and H. Fujiwara, "Universal fault diagnosis for lookup table FPGAs," *IEEE Des. Test Comput.*, vol. 15, no. 1, pp. 39–44, 1998.

[25] A. Heydari, "Revisiting approximate dynamic programming and its convergence," *IEEE Trans. Cybern.*, vol. 44, no. 12, pp. 2733–2743, Dec. 2014.

[26] M. Dubarry, C. Truchot, and B. Y. Liaw, "Synthesize battery degradation modes via a diagnostic and prognostic model," *J. Power Sources*, vol. 219, pp. 204–216, Dec. 2012.

[27] M. Broussely *et al.*, "Main aging mechanisms in Li ion batteries," *J. Power Sources*, vol. 146, no. 1–2, pp. 90–96, Aug. 2005.

[28] C. R. Birkl, M. R. Roberts, E. McTurk, P. G. Bruce, and D. A. Howey, "Degradation diagnostics for lithium ion cells," *J. Power Sources*, vol. 341, pp. 373–386, Feb. 2017.

[29] P. Verma, P. Maire, and P. Novák, "A review of the features and analyses of the solid electrolyte interphase in Li-ion batteries," *Electrochim. Acta*, vol. 55, no. 22, pp. 6332–6341, 2010.

[30] M. Kassem and C. Delacourt, "Postmortem analysis of calendar-aged graphite/$LiFePO_4$ cells," *J. Power Sources*, vol. 235, pp. 159–171, Aug. 2013.

[31] P. Keil and A. Jossen, "Calendar aging of NCA lithium-ion batteries investigated by differential voltage analysis and coulomb tracking," *J. Electrochem. Soc.*, vol. 164, no. 1, pp. A6066–A6074, Oct. 2017.

[32] M. Kerlau, M. Marcinek, V. Srinivasan, and R. M. Kostecki, "Studies of local degradation phenomena in composite cathodes for lithium-ion batteries," *Electrochim. Acta*, vol. 52, no. 17, pp. 5422–5429, May 2007.

[33] D. P. Abraham, J. L. Knuth, D. W. Dees, I. Bloom, and J. P. Christophersen, "Performance degradation of high-power lithium-ion cells—Electrochemistry of harvested electrodes," *J. Power Sources*, vol. 170, no. 2, pp. 465–475, Jul. 2007.

[34] P. Arora, R. White, and M. Doyle, "Capacity fade mechanisms and side reactions in lithium-ion batteries," *J. Electrochem. Soc.*, vol. 145, no. 10, pp. 3647–3667, 1998.

[35] P. Liu *et al.*, "Aging mechanisms of $LiFePO_4$ batteries deduced by electrochemical and structural analyses," *J. Electrochem. Soc.*, vol. 157, no. 4, pp. A499–A507, 2010.

[36] D. Anseán *et al.*, "Operando lithium plating quantification and early detection of a commercial LiFePO4 cell cycled under dynamic driving schedule," *J. Power Sources*, vol. 356, pp. 36–46, 2017.

[37] Q. Liu *et al.*, "Understanding undesirable anode lithium plating issues in lithium-ion batteries," *RSC Adv.*, vol. 6, no. 91, pp. 88683–88700, 2016.

[38] J. C. Burns *et al.*, "Predicting and extending the lifetime of Li-ion batteries," *J. Electrochem. Soc.*, vol. 160, no. 9, pp. A1451–A1456, Jul. 2013.

[39] V. Agubra and J. Fergus, "Lithium Ion battery anode aging mechanisms," *Mater. (Basel).*, vol. 6, no. 4, pp. 1310–1325, Mar. 2013.

[40] A. Barré, B. Deguilhem, S. Grolleau, M. Gérard, F. Suard, and D. Riu, "A review on lithium-ion battery ageing mechanisms and estimations for automotive applications," *J. Power Sources*, vol. 241, pp. 680–689, Nov. 2013.

[41] T. Waldmann, B.-I. Hogg, and M. Wohlfahrt-Mehrens, "Li plating as unwanted side reaction in commercial Li-ion cells—A review," *J. Power Sources*, vol. 384, pp. 107–124, Apr. 2018.

[42] Z. Li, J. Huang, B. Y. Liaw, V. Metzler, and J. Zhang, "A review of lithium deposition in lithium-ion and lithium metal secondary batteries," *J. Power Sources*, vol. 254, pp. 168–182, May 2014.

[43] A. H. Thompson, "Electrochemical potential spectroscopy: A new electrochemical measurement," *J. Electrochem. Soc.*, vol. 126, no. 4, pp. 608–616, Apr. 1979.

[44] Y. Gao and J. R. Dahn, "Synthesis and characterization of LiMnO for Li-ion battery applications," *J. Electrochem. Soc.*, vol. 143, no. 1, pp. 100–114, 1996.

[45] D. Anseán *et al.*, "Fast charging technique for high power LiFePO4 batteries: A mechanistic analysis of aging," *J. Power Sources*, vol. 321, pp. 201–209, Jul. 2016.

[46] M. Safari and C. Delacourt, "Aging of a commercial graphite/LiFePO4 cell," *J. Electrochem. Soc.*, vol. 158, no. 10, pp. A1123–1135, 2011.

[47] M. Dubarry, V. Svoboda, R. Hwu, and B. Y. Liaw, "Incremental capacity analysis and close-to-equilibrium OCV measurements to quantify capacity fade in commercial rechargeable lithium batteries," *Electrochem. Solid-State Lett.*, vol. 9, no. 10, pp. A454–A457, 2006.

[48] D. Anseán, M. González, C. Blanco, J. C. Viera, Y. Fernández, and V. M. García, "Lithium-ion battery degradation indicators via incremental capacity analysis," in *Proc. Conf. Proc.—17th IEEE Int. Conf. Environ. Electr. Eng.1st IEEE Ind. Commercial Power Syst. Europe*, 2017. Q5

[49] B. Y. Liaw and M. Dubarry, *Electric and Hybrid Vehicles, Power Sources, Models, Sustainability, Infrastructure and the Market*. Elsevier, 2010.

[50] D. Anseán, "High power Lithium-ion battery performance: A mechanistic analysis of aging," Ph.D. dissertation, University of Oviedo, Spain, 2015. Q6

[51] J. Christensen and J. Newman, "Cyclable lithium and capacity loss in Li-ion cells," *J. Electrochem. Soc.*, vol. 152, no. 4, pp. A818–A829, 2005.

[52] A. J. Smith, H. M. Dahn, J. C. Burns, and J. R. Dahn, "Long-term low-rate cycling of $LiCoO_2$ /Graphite Li-Ion cells at 55 °C," *J. Electrochem. Soc.*, vol. 159, no. 6, pp. A705–A710, 2012.

[53] M. Dubarry *et al.*, "Evaluation of commercial lithium-ion cells based on composite positive electrode for plug-in hybrid electric vehicle (PHEV) applications: IV. Over-discharge phenomena," *J. Electrochem. Soc.*, vol. 162, no. 9, pp. A1787–A1792, 2015.

[54] A. J. Smith, N. N. Sinha, and J. R. Dahn, "Narrow range cycling and storage of commercial Li Ion cells," *J. Electrochem. Soc.*, vol. 160, no. 2, pp. A235–A242, 2012.

[55] M. Klett *et al.*, "Non-uniform aging of cycled commercial LiFePO4//graphite cylindrical cells revealed by post-mortem analysis," *J. Power Sources*, vol. 257, pp. 126–137, Feb. 2014.

[56] H. M. Dahn, A. J. Smith, J. C. Burns, D. A. Stevens, and J. R. Dahn, "User-friendly differential voltage analysis freeware for the analysis of degradation mechanisms in Li-Ion batteries," *J. Electrochem. Soc.*, vol. 159, no. 9, pp. A1405–A1409, Aug. 2012.

Q7 [57] Alawa Central. (2017). [Online]. Available: https://www.soest.hawaii.edu/HNEI/alawa/

[58] D. Anseán, M. González, J. C. Viera, V. M. García, C. Blanco, and M. Valledor, "Fast charging technique for high power lithium iron phosphate batteries: A cycle life analysis," *J. Power Sources*, vol. 239, pp. 9–15, 2013.

[59] J. Schmalstieg, S. Käbitz, M. Ecker, and D. U. Sauer, "A holistic aging model for Li(NiMnCo)O_2 based 18650 lithium-ion batteries," *J. Power Sources*, vol. 257, pp. 325–334, Jul. 2014.

[60] M. Ecker *et al.*, "Calendar and cycle life study of Li(NiMnCo)O2-based 18650 lithium-ion batteries," *J. Power Sources*, vol. 248, pp. 839–851, Feb. 2014.

[61] J. Wang *et al.*, "Degradation of lithium ion batteries employing graphite negatives and nickel–cobalt–manganese oxide + spinel manganese oxide positives: Part 1, aging mechanisms and life estimation," *J. Power Sources*, vol. 269, pp. 937–948, Dec. 2014.

[62] S. F. Schuster *et al.*, "Nonlinear aging characteristics of lithium-ion cells under different operational conditions," *J. Energy Storage*, vol. 1, pp. 44–53, Jun. 2015.

[63] P. Keil and A. Jossen, "Charging protocols for lithium-ion batteries and their impact on cycle life—An experimental study with different 18650 high-power cells," *J. Energy Storage*, vol. 6, pp. 125–141, May 2016.

[64] L. E. Downie, L. J. Krause, J. C. Burns, L. D. Jensen, V. L. Chevrier, and J. R. Dahn, "In Situ detection of lithium plating on graphite electrodes by electrochemical calorimetry," *J. Electrochem. Soc.*, vol. 160, no. 4, pp. 588–594, 2013.

[65] P. Braun, J. Cho, J. Pikul, W. King, and H. Zhang, "High power rechargeable batteries," *Current Opinion Solid State Mater. Sci.*, vol. 16, pp. 186–198, 2012.

[66] M. Dubarry, M. Berecibar, A. Devie, D. Anseán, N. Omar, and I. Villarreal, "State of health battery estimator enabling degradation diagnosis: Model and algorithm description," *J. Power Sources*, vol. 360, pp. 59–69, 2017.

[67] L. Tan, L. Zhang, Q. Sun, M. Shen, Q. Qu, and H. Zheng, "Capacity loss induced by lithium deposition at graphite anode for LiFePO4/graphite cell cycling at different temperatures," *Electrochim. Acta*, vol. 111, pp. 802–808, Nov. 2013.

[68] E. Sarasketa-Zabala, F. Aguesse, I. Villarreal, L. M. Rodriguez-Martinez, C. M. López, and P. Kubiak, "Understanding lithium inventory loss and sudden performance fade in cylindrical cells during cycling with deep-discharge steps," *J. Phys. Chem. C*, vol. 119, no. 2, pp. 896–906, 2015.

[69] M. Dubarry, N. Qin, and P. Brooker, "Calendar aging of commercial Li-ion cells of different chemistries—A review," in *Current Opinion in Electrochemistry*, vol. 9. Elsevier, pp. 106–113, 2018.

[70] J. Groot, M. Swierczynski, A. I. Stan, and S. K. Kær, "On the complex ageing characteristics of high-power LiFePO4/graphite battery cells cycled with high charge and discharge currents," *J. Power Sources*, vol. 286, pp. 475–487, Jul. 2015.

[71] M. Petzl, M. Kasper, and M. A. Danzer, "Lithium plating in a commercial lithium-ion battery—A low-temperature aging study," *J. Power Sources*, vol. 275, pp. 799–807, Feb. 2015.

[72] M. C. Smart and B. V. Ratnakumar, "Effects of electrolyte composition on lithium plating in lithium-ion cells," *J. Electrochem. Soc.*, vol. 158, no. 4, pp. A379–A389, 2011.

[73] M. Petzl and M. A. Danzer, "Nondestructive detection, characterization, and quantification of lithium plating in commercial lithium-ion batteries," *J. Power Sources*, vol. 254, pp. 80–87, May 2014.

[74] S. M. Rezvanizaniani, Z. Liu, Y. Chen, and J. Lee, "Review and recent advances in battery health monitoring and prognostics technologies for electric vehicle (EV) safety and mobility," *J. Power Sources*, vol. 256, pp. 110–124, Jun. 2014.

[75] X. Xu, Z. Li, and N. Chen, "A hierarchical model for lithium-ion battery degradation prediction," *IEEE Trans. Rel.*, vol. 65, no. 1, pp. 310–325, Mar. 2016.

[76] L. Sánchez *et al.*, "Assessing the health of LiFePO4 traction batteries through monotonic echo state networks," *Sensors*, vol. 18, no. 2, p. 9, Dec. 2017.

David Anseán received the M.Eng. degree from the University of Granada, Granada, Spain, in 2007, and the Ph.D. degree (with honors) from the University of Oviedo, Spain, in 2015, both in electronics engineering.

He gained international experience (Basingstoke, U.K., and Berkeley, CA, USA) in technological companies after receiving the M.Eng. degree. After receiving the Ph.D. degree, he joined the University of Hawaii, Hawaii, USA, as a Postdoctoral Fellow, to work on advanced diagnosis and prognosis techniques on lithium-ion batteries. He joined the University of Oviedo, Spain, as an Assistant Professor in 2016. He is the Instructor of undergraduate and graduate courses including power electronics, digital integrated circuits, and embedded systems. His research interests include lithium-ion battery degradation mechanisms analysis via non-invasive methods, battery testing, and characterization, and design of battery fast charging. Q8

As a doctoral student, Dr. Anseán was the recipient of a research fellowship stay at the Electrochemical Power Systems Laboratory, at the University of Hawaii, USA. In 2018, he was the recipient of a Visiting Scholar Research Fellowship at the Institute for Power Electronics and Electrical Drives (ISEA) at RWTH Aachen University, Germany.

Víctor Manuel García Fernández received the Ph.D. degree in chemistry from the University of Oviedo, Spain.

Currently, he is an Associate Professor in the area of physical chemistry, where he teaches applied electrochemistry, centering around quantitative description of thermodynamic and kinetics phenomena in batteries and electrochemical corrosion cells. He is a member of the Battery Research Laboratory, where he collaborates in the electrochemical and thermal characterization, and modeling of Li-ion cells, and in the application of techniques, such as incremental capacity, peak area, and electrochemical impedance spectroscopy to quantify the effects of aging on materials.

Manuela González received the M.Sc. and the Ph.D. degrees in electrical engineering from the University of Oviedo, Spain, in 1992 and 1998, respectively.

She is the Founder and Head of the "Battery Research Laboratory" in the Electrical Engineering Department of University of Oviedo, a multidisciplinary team that focuses its research on the electrical and chemical characterization of batteries, the design of efficient fast-charging and management methods. She has collaborated in more than 25 R&D battery-related projects, combining the research with the transference of results to companies. With over 20 years of experience in the field of batteries, her research interests include novel Li-ion technologies for transportation and energy storage systems applications, including the development of advanced state-of-health estimation methods.

Cecilio Blanco received the M.Sc. and Ph.D. degrees in electrical engineering from the University of Oviedo, Spain, in 1989 and 1996, respectively.

Since 1989, he has been with the Department of Electrical and Electronic Engineering, University of Oviedo, where he is currently an Associate Professor and the Head of the Instrumentation and Energy Storage Systems Group. His research interests include electronic instrumentation systems, battery characterization, and modeling.

Juan Carlos Viera received the Ph.D. degree from the University of Oviedo, Spain, in 2003.

Currently, he is an Associate Professor with the Electrical and Electronics Engineering Department of the University of Oviedo. He has over 20 years of battery researching experience. He leads and collaborates with several projects, especially in the field of electric vehicles and battery energy storage systems. His research interests include energy storage systems, new advanced battery technologies, and battery management systems, focusing on the design of battery test benches, and electrical and chemical characterization under standard/stressful conditions.

Yoana Fernández Pulido received the B.Sc. degree in Chemistry from the University of Oviedo, Spain, in 2010, and the M.Sc. degree in Science and Chemistry Technology from The National Distance Education University (UNED), Madrid, Spain, in 2013. She is currently working toward the Ph.D. degree at the Battery Research Laboratory at University of Oviedo.

She worked as a Researcher with the Chemistry faculty at the University of Oviedo until 2015.

Luciano Sánchez received the M.Sc. and Ph.D. degrees in electronic engineering, from the University of Oviedo, Spain, in 1991 and 1994, respectively.

He has led 6 research projects supported by the Spanish government, 4 regional projects, and 16 privately funded research contracts. He was an external consultant for Electromateriales KLK (1991–1995), Saint-Gobain Cristalería (2000–2002), HC Energía (2003–2005), ITVASA (2005–2008), Indra Sistemas S.A. (2010–2011), Treelogic (2012–2014), GAMESA Corp (2014), Rolls-Royce Deutschland (2017), and RENFE (2018). He was also Visiting Scholar with UC Berkeley, Berkeley, CA, USA (1995), and GE Global Research (1996). He is a Professor with the Computer Science Department at the University of Oviedo, Spain. He is Head of the Research Group Metrology and Models, and Founding Partner of the spinoff of the research group IDALIA S.L. He has authored more than 70 international journals and more than 130 conference papers and book chapters, obtaining more than 4500 citations. His research interests include the theoretical study of algorithms for mathematical modeling and intelligent data analysis, and the application of these techniques to practical problems of industrial modeling, signal processing, and dimensional metrology, with special interest in the study of low-quality data.

Dr. Sánchez was the recipient of the IEEE Outstanding Paper Award in the 2013 IEEE International Conference on Fuzzy Systems (Hyderabad, India) and the 2013 Rolls-Royce Deutschland Engineering Innovationspreis (Berlin, Germany).